

DARBOUX COORDINATES FOR SYMPLECTIC GROUPOID AND CLUSTER ALGEBRAS

LEONID O. CHEKHOV* AND MICHAEL SHAPIRO**

Dedicated to the memory of great mathematician and person Boris Dubrovin

ABSTRACT. Using Fock–Goncharov higher Teichmüller space variables we derive Darboux coordinate representation for entries of general symplectic leaves of the \mathcal{A}_n groupoid of upper-triangular matrices and, in a more general setting, of higher-dimensional symplectic leaves for algebras governed by the reflection equation with the trigonometric R -matrix. The obtained results are in a perfect agreement with the previously obtained Poisson and quantum representations of groupoid variables for \mathcal{A}_3 and \mathcal{A}_4 in terms of geodesic functions for Riemann surfaces with holes. We represent braid-group transformations for \mathcal{A}_n via sequences of cluster mutations in the special \mathbb{A}_n -quiver. We prove the groupoid relations for quantum transport matrices and, as a byproduct, obtain the Goldman bracket in the semiclassical limit.

1. INTRODUCTION

1.1. Symplectic groupoid, induced Poisson structure on the unipotent upper triangular matrices. Let V denote an n -dimensional vector space, \mathcal{A} be some subspace of bilinear forms on V . Fixing the basis in V , one can identify \mathcal{A} with a subspace in the space of $n \times n$ matrices. The matrix B of a change of a basis in V takes a matrix of bilinear form $\mathbb{A} \in \mathcal{A}$ to $B\mathbb{A}B^T$.

Below we consider an important particular case when \mathcal{A} is the space of unipotent forms identified with the space of the unipotent matrices. The basis change B acts on \mathcal{A} only if the product $B\mathbb{A}B^T$ be unipotent itself. We thus introduce the space of *morphisms* identified with admissible pairs of matrices (B, \mathbb{A}) such that

$$\mathcal{M} = \{(B, \mathbb{A}) \mid B \in GL(V), \mathbb{A} \in \mathcal{A}, B\mathbb{A}B^T \in \mathcal{A}\}.$$

We then have the standard set of maps:

| | | |
|----------------|---|---|
| source | $s : \mathcal{M} \rightarrow \mathcal{A}$ | $(B, \mathbb{A}) \rightarrow \mathbb{A}$, |
| target | $t : \mathcal{M} \rightarrow \mathcal{A}$ | $(B, \mathbb{A}) \rightarrow B\mathbb{A}B^T$, |
| injection | $e : \mathcal{A} \rightarrow \mathcal{M}$ | $\mathbb{A} \rightarrow (E, \mathbb{A})$, |
| inversion | $i : \mathcal{M} \rightarrow \mathcal{M}$ | $(B, \mathbb{A}) \rightarrow (B^{-1}, B\mathbb{A}B^T)$, |
| multiplication | $m : \mathcal{M}^{(2)} \rightarrow \mathcal{M}$ | $((C, B\mathbb{A}B^T), (B, \mathbb{A})) \rightarrow (CB, \mathbb{A})$ |

*Steklov Mathematical Institute, Moscow, Russia, and Michigan State University, East Lansing, USA. Email: chekhov@msu.edu.

**Michigan State University, East Lansing, USA. Email: mshapiro@msu.edu.

such that the following diagram, where p_1 and p_2 are natural projections to the first and the second morphism in an admissible pair of morphisms, is commutative:

$$\begin{array}{ccc}
 & & \mathcal{M} \\
 & \nearrow^{p_2} & \searrow^s \\
 \mathcal{M}^{(2)} & & \mathcal{A} \\
 & \searrow_{p_1} & \nearrow_t \\
 & & \mathcal{M}
 \end{array}$$

The crucial point of the construction is the existence of a *symplectic structure*: a smooth groupoid endowed with a symplectic form $\omega \in \Omega^2\mathcal{M}$ on the morphism space \mathcal{M} that satisfies the splitting (consistency) condition [27, 42]

$$m^*\omega = p_1^*\omega + p_2^*\omega,$$

which implies, in particular, that the source and target maps Poisson commute being respectively an automorphism and an anti-automorphism of the initial Poisson algebra. Since $p_1^*\omega$ and $p_2^*\omega$ are nondegenerate, they admit a (unique) Poisson structure, and because the immersion map e is Lagrangian, this Poisson structure yields a Poisson structure on \mathcal{A} —the space of unipotent upper triangular matrices.

In 2000, Bondal [3] obtained the Poisson structure on \mathcal{A} using the algebroid construction; assuming $B = e^{\mathfrak{g}}$, we obtain the Bondal algebroid using the anchor map $D_{\mathbb{A}}$ to the tangent space $T_{\mathbb{A}}\mathcal{A}$

$$(1.1) \quad \begin{array}{ccc} D_{\mathbb{A}} : \mathfrak{g}_{\mathbb{A}} & \rightarrow & T_{\mathbb{A}}\mathcal{A} \\ & & g \mapsto \mathbb{A}g + g^T\mathbb{A}. \end{array}$$

where $\mathfrak{g}_{\mathbb{A}}$ is the linear subspace

$$\mathfrak{g}_{\mathbb{A}} := \{g \in \mathfrak{gl}_n(\mathbb{C}), | \mathbb{A} + \mathbb{A}g + g^T\mathbb{A} \in \mathcal{A}\}$$

of elements g leaving \mathbb{A} unipotent.

Lemma 1.1. [3] *The map*

$$(1.2) \quad \begin{array}{ccc} P_{\mathbb{A}} : T_{\mathbb{A}}^*\mathcal{A} & \rightarrow & \mathfrak{g}_{\mathbb{A}} \\ w & \mapsto & P_{-,1/2}(w\mathbb{A}) - P_{+,1/2}(w^T\mathbb{A}^T), \end{array}$$

where $P_{\pm,1/2}$ are the projection operators:

$$(1.3) \quad P_{\pm,1/2}a_{i,j} := \frac{1 \pm \text{sign}(j-i)}{2}a_{i,j}, \quad i, j = 1, \dots, n,$$

and $w \in T^*\mathcal{A}$ is a strictly lower triangular matrix, defines an isomorphism between the Lie algebroid $(\mathfrak{g}, D_{\mathbb{A}})$ and the Lie algebroid $(T^*\mathcal{A}, D_{\mathbb{A}}P_{\mathbb{A}})$.

The Poisson bi-vector Π on \mathcal{A} is then obtained by the anchor map on the Lie algebroid $(T^*\mathcal{A}, D_{\mathbb{A}}P_{\mathbb{A}})$ (see Proposition 10.1.4 in [31]) as:

$$(1.4) \quad \begin{array}{ccc} \Pi : T_{\mathbb{A}}^*\mathcal{A} \times T_{\mathbb{A}}^*\mathcal{A} & \mapsto & \mathcal{C}^{\infty}(\mathcal{A}) \\ (\omega_1, \omega_2) & \rightarrow & \text{Tr}(\omega_1 D_{\mathbb{A}}P_{\mathbb{A}}(\omega_2)) \end{array}$$

It can be checked explicitly that the above bilinear form is in fact skew-symmetric and gives rise to the Poisson bracket

$$(1.5) \quad \{a_{i,k}, a_{j,l}\} := \frac{\partial}{\partial a_{i,k}} \wedge \frac{\partial}{\partial a_{j,l}} \text{Tr}(da_{i,k} D_{\mathbb{A}}P_{\mathbb{A}}(da_{j,l})),$$

having the following form in components:

$$\begin{aligned}
 (1.6) \quad & \{a_{ik}, a_{jl}\} = 0, \quad \text{for } i < k < j < l, \text{ and } i < j < l < k, \\
 & \{a_{ik}, a_{jl}\} = 2(a_{ij}a_{kl} - a_{il}a_{kj}), \quad \text{for } i < j < k < l, \\
 & \{a_{ik}, a_{kl}\} = a_{ik}a_{kl} - 2a_{il}, \quad \text{for } i < k < l, \\
 & \{a_{ik}, a_{jk}\} = -a_{ik}a_{jk} + 2a_{ij}, \quad \text{for } i < j < k, \\
 & \{a_{ik}, a_{il}\} = -a_{ik}a_{il} + a_{kl}, \quad \text{for } i < k < l.
 \end{aligned}$$

This bracket turned out to coincide with the bracket previously known in mathematical physics as Gavrilik–Klimyk–Nelson–Regge–Dubrovin–Ugaglia bracket [23, 33, 34, 14, 41] and it arises from skein relations satisfied by a special finite subset of *geodesic functions* (traces of monodromies of SL_2 Fuchsian systems, which are in 1-1 correspondence with closed geodesics on a Riemann surface $\Sigma_{g,s}$) described in [7]; a simple constant log-canonical (Darboux) bracket on the space of Thurston shear coordinates z_α on the Teichmüller space $T_{g,s}$ of Riemann surfaces $\Sigma_{g,s}$ of genus g with $s = 1, 2$ holes was shown [6] to induce the above bracket on a special subset of geodesic functions identified with the matrix elements a_{ik} . All such geodesic functions admit an explicit combinatorial description [15], which immediately implies that they are Laurent polynomials with positive integer coefficients of $e^{z_\alpha/2}$. The Poisson bracket of z_α spanning the Teichmüller space $T_{g,s}$ has exactly s Casimirs, which are linear combinations of shear coordinates incident to the holes, so the subspace of z_α orthogonal to the subspace of Casimirs parameterizes a symplectic leaf in the Teichmüller space which we call a *geometric symplectic leaf*.

In [7], the Poisson embedding of geometric symplectic leaf into \mathcal{A}_n was constructed. Note however that the size n of matrix \mathbb{A}_n is related to the genus and the number of holes as $n = 2g + s$ (with s taking only two values, 1 and 2) and that the (real) dimension of $T_{g,s}$ is $6g - 6 + 3s$ increasing linearly with g whereas the total dimension of \mathcal{A}_n is obviously $n(n-1)/2$ increasing quadratically with n ; for $n = 3$ and $n = 4$ these two dimensions coincide and the geometric symplectic leaf having the dimension $6g - 6 + 2s$ is of maximum dimension.

For $n = 5$, the dimension of the geometric symplectic leaf has still the maximum value 8 of dimensions of symplectic leaves in \mathcal{A}_5 , but we have just one central element in the corresponding Teichmüller space $T_{2,1}$ and two central elements in \mathcal{A}_5 . For all larger n the dimension of geometric symplectic leaf is strictly less than the maximal dimension of symplectic leaf in \mathcal{A}_n , so the geometric systems do not describe maximal symplectic leaves in the total Poisson space of \mathcal{A}_n . The Darboux coordinates in geometric situation are well known to be the above shear coordinates, but, as just mentioned, they can not help in constructing Darboux coordinates in \mathcal{A}_n for $n \geq 5$.

The **first problem** addressed in this publication is a construction of Darboux coordinates for a general symplectic leaf of \mathcal{A}_n and explicit expression of matrix elements a_{ij} in terms of these Darboux coordinates. It was expected for long, and we show below that these Darboux coordinates are related to cluster algebras, similar to the geometric cases $n = 3, 4$.

From the integrable models standpoint, algebras (1.6) (either with a unipotent \mathbb{A}_n or with a general $\mathbb{A}_n \in \mathfrak{gl}_n$) are known under the name of *reflection equation algebras*. A task closely related to the first problem is to construct a Darboux coordinate representation for a general matrix \mathbb{A}_n enjoying the reflection equation.

1.2. Standard Poisson-Lie group \mathcal{G} and its dual. Another description of the Poisson structure on the space of triangular forms \mathcal{A} was obtained in [2]. Namely, the Poisson structure on triangular forms is a push-forward of the standard Poisson bracket on the dual group $\mathcal{G}^* = SL_n^*$ to the set of fixed points of the natural involution.

A reductive complex Lie group \mathcal{G} equipped with a Poisson bracket $\{\cdot, \cdot\}$ is called a *Poisson-Lie group* if the multiplication map $\mathcal{G} \times \mathcal{G} \ni (X, Y) \mapsto XY \in \mathcal{G}$ is Poisson. Denote by $\langle \cdot, \cdot \rangle$ an invariant nondegenerate form on the corresponding Lie algebra $\mathfrak{g} = \text{Lie}(\mathcal{G})$, and by ∇^R, ∇^L the right and left gradients of functions on \mathcal{G} with respect to this form defined by

$$\langle \nabla^R f(X), \xi \rangle = \left. \frac{d}{dt} \right|_{t=0} f(Xe^{t\xi}), \quad \langle \nabla^L f(X), \xi \rangle = \left. \frac{d}{dt} \right|_{t=0} f(e^{t\xi}X)$$

for any $\xi \in \mathfrak{g}, X \in \mathcal{G}$.

Let $\pi_{>0}, \pi_{<0}$ be projections of \mathfrak{g} onto subalgebras spanned by positive and negative roots, π_0 be the projection onto the Cartan subalgebra \mathfrak{h} , and let $R = \pi_{>0} - \pi_{<0}$. The *standard Poisson-Lie bracket* $\{\cdot, \cdot\}_r$ on \mathcal{G} can be written as

$$(1.7) \quad \{f_1, f_2\}_r = \frac{1}{2} (\langle R(\nabla^L f_1), \nabla^L f_2 \rangle - \langle R(\nabla^R f_1), \nabla^R f_2 \rangle).$$

The standard Poisson-Lie structure is a particular case of Poisson-Lie structures corresponding to quasitriangular Lie bialgebras. For a detailed exposition of these structures see, e. g., [4, Ch. 1], [37] and [43].

Following [37], let us recall the construction of *the Drinfeld double*. The double of \mathfrak{g} is $D(\mathfrak{g}) = \mathfrak{g} \oplus \mathfrak{g}$ equipped with an invariant nondegenerate bilinear form $\langle\langle (\xi, \eta), (\xi', \eta') \rangle\rangle = \langle \xi, \xi' \rangle - \langle \eta, \eta' \rangle$. Define subalgebras \mathfrak{d}_\pm of $D(\mathfrak{g})$ by $\mathfrak{d}_+ = \{(\xi, \xi) : \xi \in \mathfrak{g}\}$ and $\mathfrak{d}_- = \{(R_+(\xi), R_-(\xi)) : \xi \in \mathfrak{g}\}$, where $R_\pm \in \text{End } \mathfrak{g}$ is given by $R_\pm = \frac{1}{2}(R \pm \text{Id})$. The operator $R_D = \pi_{\mathfrak{d}_+} - \pi_{\mathfrak{d}_-}$ can be used to define a Poisson-Lie structure on $D(\mathcal{G}) = \mathcal{G} \times \mathcal{G}$, the double of the group \mathcal{G} , via

$$(1.8) \quad \{f_1, f_2\}_D = \frac{1}{2} (\langle\langle R_D(\nabla^L f_1), \nabla^L f_2 \rangle\rangle - \langle\langle R_D(\nabla^R f_1), \nabla^R f_2 \rangle\rangle),$$

where ∇^R and ∇^L are right and left gradients with respect to $\langle\langle \cdot, \cdot \rangle\rangle$. The diagonal subgroup $\{(X, X) : X \in \mathcal{G}\}$ is a Poisson-Lie subgroup of $D(\mathcal{G})$ (whose Lie algebra is \mathfrak{d}_+) naturally isomorphic to $(\mathcal{G}, \{\cdot, \cdot\}_r)$.

The group \mathcal{G}^* whose Lie algebra is \mathfrak{d}_- is a Poisson-Lie subgroup of $D(\mathcal{G})$ called *the dual Poisson-Lie group of \mathcal{G}* . The Poisson bracket $\{\cdot, \cdot\}_D$ induces the Poisson bracket on \mathcal{G}^* .

For $\mathcal{G} = SL_n$ the dual group $\mathcal{G}^* = \{(X_+, Y_-)\} \in B_+ \times B_-$ satisfying the additional relation $\pi_0(X_+)\pi_0(Y_-) = \text{Id}$ where $B_+(B_-) \subset SL_n$ are Borel subgroups of nondegenerate upper (lower) triangular matrices.

The involution $\iota_{\mathcal{G}^*} : \mathcal{G}^* \rightarrow \mathcal{G}^*$ takes (X_+, Y_-) to (Y_-^t, X_+^t) .

The subgroup \mathcal{U}_+ of unipotent upper triangular matrices is embedded diagonally in \mathcal{G}^* . The embedding $\epsilon : \mathcal{U}_+ \hookrightarrow \mathcal{G}^*$ maps $X \in \mathcal{U}_+$ to (X, X) . The image $\epsilon(\mathcal{U}_+)$ is the set of fixed points of involution $\iota_{\mathcal{G}^*}$.

The image $\epsilon(\mathcal{U}_+)$ is not a Poisson subvariety of \mathcal{G}^* however the Dirac reduction induces the Poisson bi-vector Π (1.4) on \mathcal{U}_+ .

For sake of completeness, we remind here the definition of Dirac reduction. Let X be a subvariety of a Poisson variety $(V, \{\cdot, \cdot\}_{PB})$ defined by constrains $\phi_i = \text{const}$. The second class constrains are constrains $\tilde{\phi}_a$ which have nonvanishing Poisson bracket with at least one other constraint.

Define matrix U with entries $U_{ab} = \{\tilde{\phi}_a, \tilde{\phi}_b\}_{PB}$. Note that U is always invertible.

Then, Dirac bracket of functions f and g on X is

$$\{f, g\}_{DB} = \{f, g\}_{PB} - \sum_{a,b} \{f, \tilde{\phi}_a\}_{PB} U_{ab}^{-1} \{\tilde{\phi}_b, g\}_{PB},$$

see [26] for details.

in a quiver still to be constructed that produces the above braid-group transformation for a generic symplectic leaf of \mathcal{A}_n .

We solve the both formulated problems in this paper: we explicitly construct the quiver (called an \mathbb{A}_n -quiver) such that the entries $a_{i,j}$ of the unipotent matrix \mathbb{A} are positive Laurent polynomials of the cluster quiver variables, construct a quantum version of this quiver thus realizing the representation (1.11) and finding explicitly chains of mutations of the \mathbb{A}_n -quiver that produce the braid-group transformations.

1.4. Cluster algebra and cluster mutations. Cluster algebras were introduced in [21] by S.Fomin and A.Zelevinsky in 2001 in an effort to describe (dual) canonical basis of the (quantized) universal enveloping algebra. Cluster algebra is determined by combinatorial *cluster structures* consisting of (infinite) set of seeds and mutation rules. Each seed (of cluster algebra of geometric type) consists of the collection of n cluster variables X_i , $i \in [1, n]$ (elements of quantum torus (see Section 2.2 for detailed description)) and an $n \times n$ integer skew-symmetric exchange matrix B . Seeds are connected by mutations. Each cluster algebra is equipped with the compatible Poisson structure [24] and allows quantization [1].

For $k \in [1, n]$ a quantum cluster mutation μ_k is defined as the following transformations of seed (see [18])

$$\mu_k(X_j) = \begin{cases} X_k^{-1}, & \text{if } j = k \\ X_j \left(\prod_{a=1}^{|b_{jk}|} (1 + q^{2a-1} X_k^{-\text{sgn}(b_{jk})}) \right)^{-b_{jk}}, & \text{otherwise.} \end{cases}$$

Mutation of exchange matrix is described by $\mu_k(b_{ij}) = \begin{cases} -b_{ij}, & \text{if } i = k \text{ or } j = k; \\ b_{ij} + \frac{b_{ik}|b_{kj}| + |b_{ik}|b_{kj}}{2}, & \text{otherwise.} \end{cases}$

An integer skew-symmetric $n \times n$ matrix is encoded by exchange quiver with n vertices labeled 1 to n and multiple arrows. If $k, \ell \in [1, n]$ are indices such that $b_{k\ell} > 0$ then vertex k is connected to ℓ by $b_{k\ell}$ arrows. Exchange matrix mutations correspond to mutations of exchange quiver.

2. SL_n -ALGEBRAS FOR THE TRIANGLE $\Sigma_{0,1,3}$

Let $\Sigma_{g,s,p}$ denote a topological genus g surface with s boundary components and p marked points. In what follows, we concentrate on the case of the disk with 3 marked points on the boundary $\Sigma_{0,1,3}$. (To simplify notations, we use $\Sigma = \Sigma_{0,1,3}$.) In this section we review the definition of quantized moduli space $\mathcal{X}_{SL_n, \Sigma}$ closely related to the SL_n -local systems on the disk with three marked points ([16]). We call disk with three marked points a, b, c *triangle with vertices a, b, c* and use notation S_{abc} (see Fig 1).

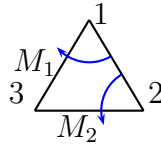


FIGURE 1. Triangle $S_{1,2,3}$ with vertices 1, 2, 3.

2.1. Moduli space $\mathcal{X}_{SL_n, \Sigma}$ and transport matrices. Following [16], recall that a moduli space $\mathcal{X}_{SL_n, \Sigma}$ parametrizes SL_n -local systems on Σ or, equivalently, triples of flags in \mathbb{C}^n in general position. Any SL_n -local system in the triangle S_{123} determines *monodromy* (or *transport*) matrices.

Two transport matrices M_1 and M_2 correspond respectively to directed paths going from one side of Σ to the other side as on Fig 1. If M is associated to a directed path then the inverse matrix M^{-1} corresponds to the same path in the opposite direction.

Consider a triple of flags in general position $(F_1)_\bullet, (F_2)_\bullet, (F_3)_\bullet$ in \mathbb{C}^n . Recall that a *complete flag* F_\bullet is a collection of consecutively embedded subspaces $\{0 = F_0 \subset F_1 \subset \dots \subset F_k \subset \dots \subset F_{n-1} \subset F_n = \mathbb{C}^n\}$ where F_k is a linear subspace of dimension k . Denote by $F^a = F_{n-a}$, $a = 0, 1, \dots, n$, the vector subspace of codimension a .

Flag $(F_i)_\bullet$ is assigned to vertex i of triangle S_{123} , for all $i \in [1, 3]$. Consider the subtriangulation of S_{123} into $\binom{n}{2}$ white upright triangles and $\binom{n-1}{2}$ upside-down black triangles (see Fig. 2). Label all white upright triangles by triples $\{(a, b, c) | a, b, c \geq 0 \& a + b + c = n - 1\}$ such that subtriangle $(n - 1, 0, 0)$ is closer to vertex 1 of S_{123} , subtriangle $(0, n - 1, 0)$ is closer to vertex 2 and subtriangle $(0, 0, n - 1)$ is closer to vertex 3. Each white triangle (a, b, c) corresponds to a line $\ell_{abc} = (F_1)^a \cap (F_2)^b \cap (F_3)^c$. Similarly, label black upside-down triangles by triples $\{(abc) | a, b, c \geq 0 \& a + b + c = n - 2\}$ where the labels satisfy similar agreement as labels of white subtriangles. Each upside-down (black) triangle (α, β, γ) is associated with the plane $P_{abc} = (F_1)^a \cap (F_2)^b \cap (F_3)^c$. Note that every plane P_{abc} of a black triangle contains all three lines $\ell_{(a+1)bc}, \ell_{a(b+1)c}, \ell_{ab(c+1)}$ of white triangles which are neighbors of the black one. For every such plane P_{abc} choose three vectors $\mathbf{v}_{(a+1)bc} \in \ell_{(a+1)bc}$, $\mathbf{v}_{a(b+1)c} \in \ell_{a(b+1)c}$, $\mathbf{v}_{ab(c+1)} \in \ell_{ab(c+1)}$ such that they satisfy condition $\mathbf{v}_{(a+1)bc} + \mathbf{v}_{a(b+1)c} = \mathbf{v}_{ab(c+1)}$. Hence, given a configuration of lines corresponding to triple of flags $((F_1)_\bullet, (F_2)_\bullet, (F_3)_\bullet)$, the choice of one vector $\mathbf{v}_{abc} \in \ell_{abc}$ determines uniquely all other vectors in the lines $\ell_{a'b'c'}$ for all $(a'b'c')$ (see Fig. 3).

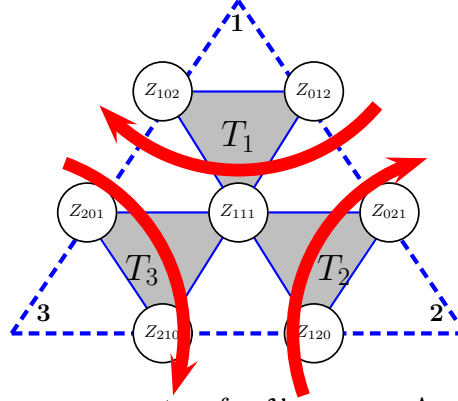


FIGURE 2. Fock-Goncharov parameters for $\mathcal{X}_{SL_3, \Sigma_{0,1,3}}$. Arrows shows the direction of transport matrices. $M_1 = T_1$, $M_2 = T_2^{-1}$.

Thus, the configuration of lines ℓ_{abc} determines *projective collection of vectors* $\{\mathbf{v}_{abc}\}$ modulo scalar scaling. Note that exactly two vectors at vertices of any gray triangle are independent.

Define a snake as an oriented path connecting the top line ℓ_{n00} downwards to the bottom ℓ_{0ab} (red path in Fig 3 is an example of a snake).

Any snake defines a projective basis $\mathbf{v}_{\alpha_1}, \dots, \mathbf{v}_{\alpha_n}$ of \mathbb{C}^n . Note that changing orientation replaces the basis to opposite one $\mathbf{v}_{\alpha_n}, -\mathbf{v}_{\alpha_{n-1}}, \dots, (-1)^{n-1}\mathbf{v}_{\alpha_1}$. For instance, the red snake top to bottom in Fig. 3 defines the basis $\mathbf{v}_{200}, \mathbf{v}_{110}, \mathbf{v}_{011}$.

Denote by \mathbf{b}_p the basis defined by snake p . Let \mathbf{b}_{12} be the basis defined by the unique snake from ℓ_{n00} to ℓ_{0n0} in the triangle S_{123} and by \mathbf{b}_{31} the basis defined by the snake ℓ_{00n} to ℓ_{n00} . The basis \mathbf{b}_{12} in Fig 4 is $\mathbf{b}_{12} = (\mathbf{v}_{200}, \mathbf{v}_{110}, \mathbf{v}_{020})$, the basis $\mathbf{b}_{31} = (\mathbf{v}_{002}, \mathbf{v}_{101}, \mathbf{v}_{200})$. Note that the snake and the basis depends on the triangle in which the snake is considered. The basis associated with the red snake in the triangle S_{125} (see Fig. 4) is $\mathbf{b}'_{12} = \{(\mathbf{v}'_{200}, \mathbf{v}'_{110}, \mathbf{v}'_{020})\}$. Note that vectors $\mathbf{v}_{abc} \in \mathbf{b}_{12}$ and $\mathbf{v}'_{abc} \in \mathbf{b}'_{12}$ are scalar multiple of each other. Similarly, we consider

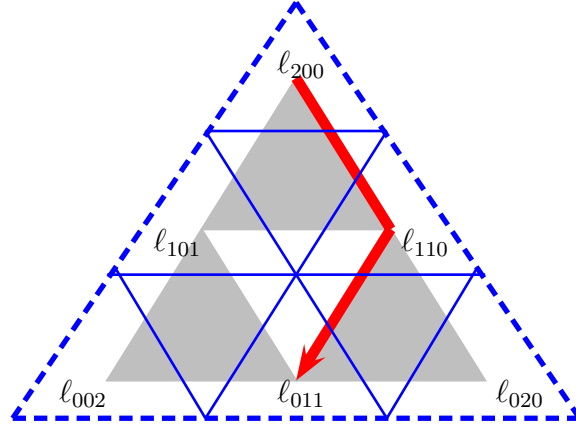


FIGURE 3. Configuration of lines corresponding to triple of flags in \mathbb{C}^3 . Black triangles are equipped with planes P_{abc} . Plane P_{100} contains lines $l_{200}, l_{110}, l_{101}$, P_{010} contains lines $l_{110}, l_{020}, l_{011}$, P_{001} contains lines $l_{101}, l_{011}, l_{002}$. Vectors $\mathbf{v}_{abc} \in l_{abc}$ satisfy relations $\mathbf{v}_{101} = \mathbf{v}_{200} + \mathbf{v}_{110}$, $\mathbf{v}_{020} = \mathbf{v}_{101} + \mathbf{v}_{011}$, $\mathbf{v}_{011} = \mathbf{v}_{110} + \mathbf{v}_{002}$.

the basis $\mathbf{b}''_{31} = (\mathbf{v}''_{002}, \mathbf{v}''_{101}, \mathbf{v}''_{200})$ associated with the snake in S_{134} ; vector $\mathbf{v}''_{abc} \in \mathbf{b}''_{31}$ is a scalar multiple of the vector $\mathbf{v}_{abc} \in \mathbf{b}_{31}$.

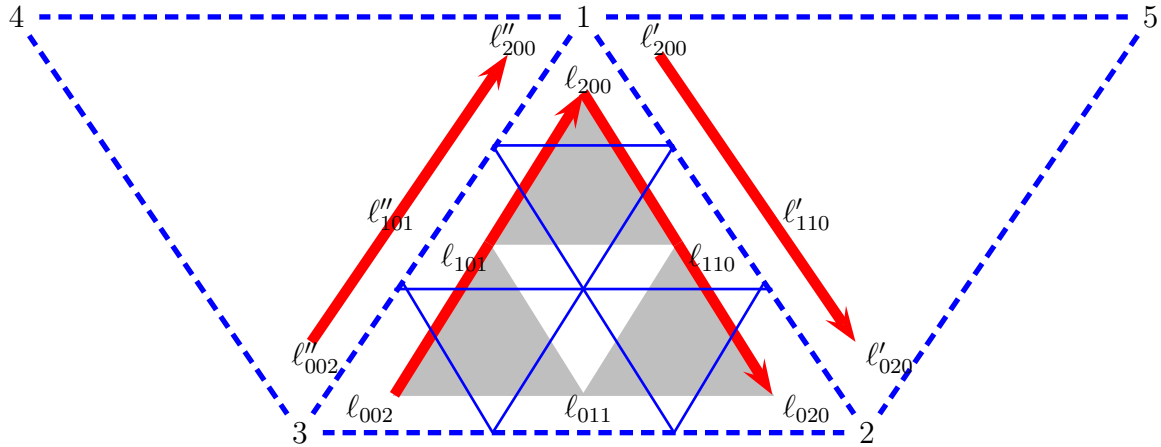


FIGURE 4. Configuration of lines corresponding to triple of flags in \mathbb{C}^3 . Black triangles are equipped with planes P_{abc} . Plane P_{100} contains lines $l_{200}, l_{110}, l_{101}$, P_{010} contains lines $l_{110}, l_{020}, l_{011}$, P_{001} contains lines $l_{101}, l_{011}, l_{002}$. Vectors $\mathbf{v}_{abc} \in l_{abc}$ satisfy relations $\mathbf{v}_{101} = \mathbf{v}_{200} + \mathbf{v}_{110}$, $\mathbf{v}_{020} = \mathbf{v}_{101} + \mathbf{v}_{011}$, $\mathbf{v}_{011} = \mathbf{v}_{110} + \mathbf{v}_{002}$. Lines in triangle S_{125} are denoted by l'_{abc} , line in triangle S_{135} are denoted by l''_{abc} .

Define $T_1 \in SL_n$ as the transformation matrix from basis \mathbf{b}''_{31} to \mathbf{b}'_{12} , namely, i -th column of T_1 is $[(\mathbf{b}''_{31})_i]_{\mathbf{b}'_{12}}$, i.e. coordinate vector $(\mathbf{b}''_{31})_i$ with respect to basis \mathbf{b}'_{12} . Because \mathbf{b}''_{31} and \mathbf{b}'_{12} are both defined up to multiplicative scalars, T_1 is defined up to scalar too. Hence, condition $T_1 \in SL_n$ fixes T_1 uniquely.

Similarly, we define the transport matrix T_2 as transformation matrix from basis \mathbf{b}'_{12} to \mathbf{b}'''_{23} and T_3 as transformation from \mathbf{b}'''_{23} to \mathbf{b}''_{31} , where \mathbf{b}'''_{23} corresponds to the snake in the triangle sharing the common side 2 – 3 with S_{123} .

Finally, let $M_1 = T_1$, $M_2 = T_2^{-1}$ (see Fig. 2).

Matrix M_1 is an upper-anti-diagonal matrix and M_2 is a lower-anti-diagonal matrix (see Example 2.2).

Fock-Goncharov coordinates Z_α parametrize $\mathcal{X}_{SL_n, \Sigma}$. They are associated with vertices of triangular subdivision of Σ except vertices 1, 2, 3 of triangle and labelled using barycentric indices $(i, j, k), i + j + k = n$ denoted often below by Greek letters (see Fig. 2 for $n = 3$ and Fig. 6 for $n = 6$). The expressions for classical transport matrices were first found in [19], (see also [13] Appendix A.2).

One can factorize the transport matrix T_1 in a sequence of elementary basis changes corresponding to the following sequence of snake transformations.

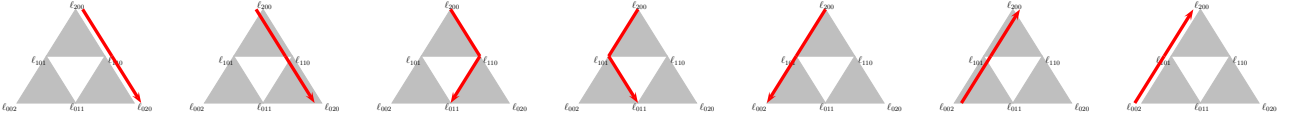


FIGURE 5. Sequence of snakes factorizing transport matrix T_1

Let $\chi(k)$ denote the integer step function, $\chi(k) = 0$, if $k < 0$, and 1, if $k \geq 0$. Define $n \times n$ matrices $H_k(t)$, L_k , S as follows $H_k(t) = t^{-\frac{n-k}{n}} \text{diag}(t^{\chi(1-k-1)}, t^{\chi(2-k-1)}, \dots, t^{\chi(n-k-1)})$, $L_k = \text{Id}_n + E_k$ for $k \in [1, n-1]$ where Id_n is the identity $n \times n$ matrix, $(E_k)_{i,j} = \delta_{k+1,i} \cdot \delta_{k,j}$ is the matrix whose only nonzero element is 1 at the position $(k+1, k)$, $(S)_{ij} = (-1)^{n-i} \delta_{i, n+1-j}$. Then,

$$T_1 = S \left[\prod_{j=1}^{n-1} H_{n-j}(Z_{j,0,n-j}) \right] \cdot L_{n-1} \prod_{p=1}^{n-2} \left[\left[\prod_{q=1}^p L_{n-q-1} H_{n-q}(Z_{n-q,p+q+1-n,n-1-p}) \right] L_{n-1} \right] \cdot \left[\prod_{j=1}^{n-1} H_j(Z_{j,n-j,0}) \right].$$

Here, the factor $L_{n-1} \prod_{p=1}^{n-2} \left[\left[\prod_{q=1}^p L_{n-q-1} H_{n-q}(Z_{n-q,p+q+1-n,n-1-p}) \right] L_{n-1} \right]$ is a transformation from the basis \mathbf{b}_{13} to \mathbf{b}_{12} ; $\prod_{j=1}^{n-1} H_j(Z_{j,0,n-j})$ is a transformation from \mathbf{b}_{12} to \mathbf{b}'_{12} ; finally, $S \left[\prod_{j=1}^{n-1} H_{n-j}(Z_{j,0,n-j}) \right]$ is a transformation from \mathbf{b}'_{31} to \mathbf{b}_{13} .

Let $\mathbb{I} = \{(a, b, c) | a, b, c \in \mathbb{Z}_+, a + b + c = n\}$ be the set of barycentric indices in the triangle with side n , $\tau : \mathbb{I} \rightarrow \mathbb{I}$ be the clockwise rotation by $2\pi/3$, τ acts naturally on the sequences of barycentric parameters and hence on sequences of Fock-Goncharov parameters: for $\mathbf{Z} = (Z_{\alpha_1}, \dots, Z_{\alpha_k})$ the sequence $\tau \mathbf{Z} = (Z_{\tau(\alpha_1)}, \dots, Z_{\tau(\alpha_k)})$, for any object $O(\mathbf{Z})$ depending on the collection $\mathbf{Z} = (Z_{\alpha_i})_{i=1}^k$ we set $\tau O = O(\tau \mathbf{Z})$.

Note that $T_2 = \tau T_1$, $T_3 = \tau^2 T_1$ (see Fig. 2). The transport matrix $M_2 = (\tau M_1)^{-1}$.

Example 2.1. For $n = 3$, we have $H_1(t) = \begin{pmatrix} t^{-2/3} & 0 & 0 \\ 0 & t^{1/3} & 0 \\ 0 & 0 & t^{1/3} \end{pmatrix}$, $H_2(t) = \begin{pmatrix} t^{-1/3} & 0 & 0 \\ 0 & t^{-1/3} & 0 \\ 0 & 0 & t^{2/3} \end{pmatrix}$,

$$L_1 = \begin{pmatrix} 1 & 0 & 0 \\ 1 & 1 & 0 \\ 0 & 0 & 1 \end{pmatrix}, L_2 = \begin{pmatrix} 1 & 0 & 0 \\ 0 & 1 & 0 \\ 0 & 1 & 1 \end{pmatrix}, S = \begin{pmatrix} 0 & 0 & 1 \\ 0 & -1 & 0 \\ 1 & 0 & 0 \end{pmatrix}.$$

Transport matrices T_1 from side 1 – 2 to side 3 – 1, T_2 from side 2 – 3 to side 1 – 2 and T_3 from side 3 – 1 to side 2 – 3 (see Fig. 2) have the following form

$$\begin{aligned} M_1 = T_1 &= SH_2(Z_{201})H_1(Z_{102})L_2L_1H_2(Z_{111})L_2H_1(Z_{012})H_2(Z_{021}) \\ T_2 &= SH_2(Z_{120})H_1(Z_{210})L_2L_1H_2(Z_{111})L_2H_1(Z_{012})H_2(Z_{021}) \\ T_3 &= SH_2(Z_{021})H_1(Z_{012})L_2L_1H_2(Z_{111})L_2H_1(Z_{102})H_2(Z_{201}). \end{aligned}$$

Then, M_1 is the matrix

$$\begin{pmatrix} Z_{021}^{-1/3} Z_{102}^{1/3} Z_{111}^{-1/3} Z_{012}^{-2/3} Z_{201}^{2/3} & Z_{021}^{-1/3} Z_{102}^{1/3} (Z_{111}^{-1/3} + Z_{111}^{2/3}) Z_{102}^{1/3} Z_{201}^{2/3} & Z_{021}^{2/3} Z_{102}^{1/3} Z_{111}^{2/3} Z_{012}^{1/3} Z_{201}^{2/3} \\ Z_{021}^{-1/3} Z_{102}^{-1/3} Z_{111}^{-1/3} Z_{012}^{-2/3} Z_{201}^{-1/3} & Z_{021}^{-1/3} Z_{102}^{-1/3} Z_{111}^{-1/3} Z_{012}^{1/3} Z_{201}^{-1/3} & 0 \\ Z_{021}^{-1/3} Z_{102}^{-2/3} Z_{111}^{-1/3} Z_{012}^{-2/3} Z_{201}^{-1/3} & 0 & 0 \end{pmatrix}.$$

Recall, $M_2 = T_2^{-1}$. We can easily factorize M_2 in the product of elementary matrices noting that $S^{-1} = (-1)^{n-1} S$, $H_k(t)^{-1} = H_k(t^{-1}) = S H_{n-k}(t) S$, $L_k^{-1} = \text{Id}_n - E_k = S L_{n-k}^t S$, where L_j^t is the transpose of matrix L_j . Therefore,

$$\begin{aligned} M_2 &= H_2(Z_{210})^{-1} H_1(Z_{120})^{-1} L_2^{-1} H_2(Z_{111})^{-1} L_1^{-1} L_2^{-1} H_1(Z_{021})^{-1} H_2(Z_{012})^{-1} S^{-1} \\ &= S H_1(Z_{210}) S S H_2(Z_{120}) S S L_1^t S S H_1(Z_{111}) S S L_2^t S S L_1^t S S H_2(Z_{021}) S S H_1(Z_{012}) S S (-1)^{n-1} \\ &= (-1)^{n-1} S H_1(Z_{210}) H_2(Z_{120}) L_1^t H_1(Z_{111}) L_2^t L_1^t H_2(Z_{021}) H_1(Z_{012}). \end{aligned}$$

Then, M_2 is the following matrix

$$\begin{pmatrix} 0 & 0 & Z_{210}^{1/3} Z_{111}^{1/3} Z_{012}^{1/3} Z_{120}^{2/3} Z_{021}^{2/3} \\ 0 & Z_{210}^{1/3} Z_{111}^{1/3} Z_{012}^{1/3} Z_{120}^{-1/3} Z_{021}^{-1/3} & Z_{210}^{1/3} Z_{111}^{1/3} Z_{012}^{1/3} Z_{120}^{-1/3} Z_{021}^{2/3} \\ Z_{210}^{-2/3} Z_{111}^{-2/3} Z_{012}^{-2/3} Z_{120}^{-1/3} Z_{021}^{-1/3} & Z_{210}^{-2/3} (Z_{111}^{-2/3} + Z_{111}^{1/3}) Z_{012}^{1/3} Z_{120}^{-1/3} Z_{021}^{-1/3} & Z_{210}^{-2/3} Z_{111}^{1/3} Z_{012}^{1/3} Z_{120}^{-1/3} Z_{021}^{2/3} \end{pmatrix}.$$

To obtain quantum transport matrices we need to expand all entries of classical transport matrix M_i in the sum of monomials m_j and then replace all m_j by the corresponding Weyl form $\bullet m_j \bullet$. For instance, the $(1, 2)$ -entry of quantum M_1 becomes

$$(M_1)_{12} = \bullet Z_{021}^{-1/3} Z_{102}^{1/3} Z_{111}^{-1/3} Z_{102}^{1/3} Z_{201}^{2/3} \bullet + \bullet Z_{021}^{-1/3} Z_{102}^{1/3} Z_{111}^{2/3} Z_{102}^{1/3} Z_{201}^{2/3} \bullet$$

In Section 2.3 we generalize this construction to (quantum) non-normalized quantum transport matrices that can be defined for more general class of planar quivers.

Example 2.2. A toy example is the one in which all Z_α are the units. Matrix entries then just count numbers of monomials entering the corresponding matrix elements $a_{i,j} \in (-1)^{i+1} \mathbb{Z}_+[[Z_\alpha^{\pm 1}]]$. Then, for the M_1 matrix, we have the following representation:

$$(2.1) \quad M_1 = \begin{pmatrix} 1 & 2 & 1 \\ -1 & -1 & 0 \\ 1 & 0 & 0 \end{pmatrix}, \quad \begin{pmatrix} 1 & 3 & 3 & 1 \\ -1 & -2 & -1 & 0 \\ 1 & 1 & 0 & 0 \\ -1 & 0 & 0 & 0 \end{pmatrix}, \text{ etc,}$$

that is, $[M_1]_{i,j} = (-1)^{i+1} \begin{bmatrix} n-i \\ j \end{bmatrix}$ for SL_n . We introduce the antidiagonal unit matrix $|S| = \delta_{i,n+1-i}$ (to distinguish it from $S = (-1)^{i+1} \delta_{i,n+1-i}$).

For M_2 we have

$$(2.2) \quad M_2 = M_1^2 = \begin{pmatrix} 0 & 0 & 1 \\ 0 & -1 & -1 \\ 1 & 2 & 1 \end{pmatrix}, \quad \begin{pmatrix} 0 & 0 & 0 & 1 \\ 0 & 0 & -1 & -1 \\ 0 & 1 & 2 & 1 \\ -1 & -3 & -3 & -1 \end{pmatrix}, \text{ etc}$$

A riddle-thirsty reader can check the following relations between these matrices:

$$M_1^2 = M_2 = (-1)^{n+1} |S| \cdot M_1 \cdot |S|, \quad M_1^3 = (-1)^{n+1} [|S| \cdot M_1]^2 = (-1)^{n+1} I$$

$$(2.3) \quad M_1^T M_2 = \mathbb{A} = \begin{pmatrix} 1 & 3 & 3 \\ 0 & 1 & 3 \\ 0 & 0 & 1 \end{pmatrix}, \quad \begin{pmatrix} 1 & 4 & 6 & 4 \\ 0 & 1 & 4 & 6 \\ 0 & 0 & 1 & 4 \\ 0 & 0 & 0 & 1 \end{pmatrix}, \quad \text{etc}$$

that is $[\mathbb{A}]_{i,j} = \begin{bmatrix} n \\ j-i \end{bmatrix}$.

2.2. Quantum torus. Let lattice $\Lambda = \mathbb{Z}^n$ be equipped with a skew-symmetric integer form $\langle \cdot, \cdot \rangle$. Introduce the q -multiplication operation in the vector space $\Upsilon = \text{Span}\{Z_\lambda\}_{\lambda \in \Lambda}$ as follows $Z_\lambda Z_\mu = q^{\langle \lambda, \mu \rangle} Z_{\lambda+\mu}$. The algebra Υ is called a *quantum torus*. Fix a basis $\{e_i\}$ in Λ , we consider Υ as a non-commutative algebra of Laurent polynomials in variables $Z_i := Z_{e_i}$, $i \in [1, N]$. For any sequence $\mathbf{a} = (a_1, \dots, a_t)$, $a_i \in [1, N]$, let $\Pi_{\mathbf{s}}$ denote the monomial $\Pi_{\mathbf{s}} = Z_{a_1} Z_{a_2} \dots Z_{a_t}$. Let $\lambda_{\mathbf{s}} = \sum_{j=1}^t e_{a_j}$. Element $Z_{\lambda_{\mathbf{s}}}$ is called in physical literature the Weyl form of $\Pi_{\mathbf{s}}$ and we denote it by two-sided colons $\bullet \Pi_{\mathbf{s}} \bullet$. It is easy to see that $\bullet \Pi_{\mathbf{s}} \bullet = Z_{\lambda_{\mathbf{s}}} = q^{-\sum_{j < k} \langle e_j, e_k \rangle} \Pi_{\mathbf{s}}$.

2.3. Quantum transport matrices and quantum Fock-Goncharov coordinates. Quantum transport matrices were introduced in [39]. We describe now how quantized transport matrices are expressed in terms of quantum Fock-Goncharov parameters (see also [13], [17] and [39]).

The quantum Fock-Goncharov variables form a quantum torus Υ with commutation relation described by the quiver shown on Fig. 6. Vertices of the quiver label quantum Fock-Goncharov coordinates Z_α (we use Greek letters to indicate barycentric labels) while the arrows encode commutation relations: if there are m arrows from vertex α to β then $Z_\beta Z_\alpha = q^{-2m} Z_\alpha Z_\beta$. Dashed arrow counts as $m = 1/2$. In particular, a solid arrow from Z_α to Z_β implies $Z_\beta Z_\alpha = q^{-2} Z_\alpha Z_\beta$, a dashed arrow from Z_α to Z_β implies $Z_\beta Z_\alpha = q^{-1} Z_\alpha Z_\beta$, and, for the future use, a double arrow from Z_α to Z_β means $Z_\beta Z_\alpha = q^{-4} Z_\alpha Z_\beta$. Vertices not connected by an arrow commute.

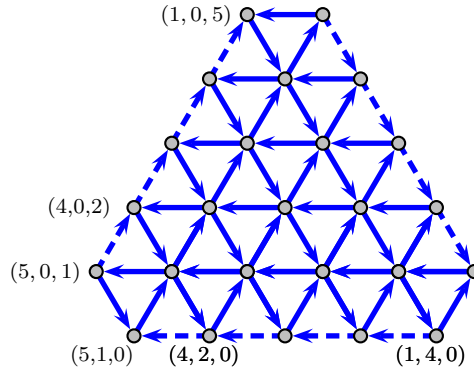


FIGURE 6. The quiver of Fock-Goncharov parameters for $n = 6$; note that vertices $(6, 0, 0)$, $(0, 6, 0)$, and $(0, 0, 6)$ are missing.

Consider the following planar oriented graph in the triangle S_{123} dual to the quiver above. Label vertices on the left, on the right and on the bottom sides from 1 to n as shown on the Figure 7. Barycentric indices label the vertices of the quiver which correspond to the faces of the dual oriented graph. Vertices of the new dual graph are colored black and white depending on whether there are inside a upright or upside-down triangle. Note that black vertex has two incoming arrows while white one has only one incoming arrow. Faces of G are equipped with q -commuting weights Z_α . We add also three face weights $Z_{n,0,0}$, $Z_{0,n,0}$, and $Z_{0,0,n}$ with the corresponding commutation relations (shown in red on Fig. 7).

Any maximal oriented path in the dual graph connects a vertex on the right side 1–2 of the triangle either with a vertex of the left side 1–3 or with a vertex on the bottom side 2–3. We

assign to every oriented path $P : j \rightsquigarrow i'$ from the right side to the left side or to the bottom side $P : j \rightsquigarrow i''$ the quantum weight $w(P) = \bullet \prod_{\substack{\text{face } \alpha \text{ lies to the right} \\ \text{of the path } P}} Z_\alpha \bullet$

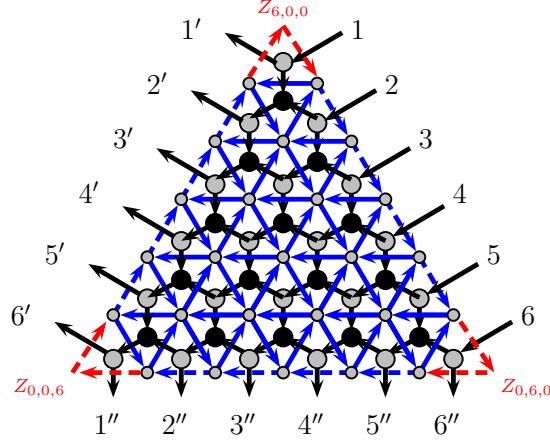


FIGURE 7. The oriented planar graph G dual to the quiver of Fock-Goncharov parameters for $\mathcal{X}_{SL_6, \Sigma}$. Additional face weights $Z_{6,0,0}, Z_{0,6,0}, Z_{0,0,6}$ are painted red.

Definition 2.3. We define two $n \times n$ non-normalized quantum transition matrices

$$(\mathcal{M}_1)_{i,j} = \sum_{\substack{\text{directed path } P:j \rightsquigarrow i' \\ \text{from right to left}}} w(P) \quad \text{and} \quad (\mathcal{M}_2)_{i,j} = \sum_{\substack{\text{directed path } P:j \rightsquigarrow i'' \\ \text{from right to bottom}}} w(P).$$

Note that each \mathcal{M}_1 is a lower-triangular matrix and \mathcal{M}_2 is an upper-triangular matrix.

In section 7.2 we generalize this definition. Let Γ be a planar oriented graph in the rectangle with no sources or sinks inside (see Fig 28), m univalent boundary sinks on the left labeled 1 to m top to bottom and n univalent boundary sources on the right labelled 1 to n top to bottom. All arrows of Γ are oriented right to left, in particular, Γ has no oriented cycles. Note that this condition is, in particular, satisfied by the oriented planar graph G (see Fig 7) considered as a graph with n sources and $2n$ sinks. Indeed, we can redraw G in a rectangle such that the right side of the triangle becomes the right vertical side of the rectangle while union of the left and the bottom sides becomes the left side of the triangle.

Faces of Γ are equipped with q -commuting weights Z_α whose commutation relations are governed by the dual quiver (see Section 7.2 for details). We define weight of the maximal oriented path P from a source a to a sink b as

$$(2.4) \quad w(P) = \bullet \prod_{\substack{\text{face } \alpha \text{ lies to the right} \\ \text{of the path } P}} Z_\alpha \bullet.$$

Then, entries of a $m \times n$ non-normalized transport matrix are $[\mathcal{M}]_{ij} = \sum_{\text{directed path } P:j \rightsquigarrow i} w(P)$.

Lemma 7.18 implies that the matrix \mathcal{M} satisfies the quantum R -matrix relation $\mathcal{R}_m(q) \overset{1}{\mathcal{M}} \otimes \overset{2}{\mathcal{M}} = \overset{2}{\mathcal{M}} \otimes \overset{1}{\mathcal{M}} \mathcal{R}_n(q)$, where $\mathcal{R}_k(q)$ is a $k^2 \times k^2$ matrix

$$(2.5) \quad \mathcal{R}_k(q) = \sum_{1 \leq i, j \leq k} \overset{1}{e}_{ii} \otimes \overset{2}{e}_{jj} + (q-1) \sum_{1 \leq i \leq k} \overset{1}{e}_{ii} \otimes \overset{2}{e}_{ii} + (q-q^{-1}) \sum_{1 \leq j < i \leq k} \overset{1}{e}_{ij} \otimes \overset{2}{e}_{ji}$$

Note that \mathcal{R}_k has the following properties:

$$(2.6) \quad \mathcal{R}_k^{-1}(q) = \mathcal{R}_k(q^{-1}), \quad \mathcal{R}_k(q) - \mathcal{R}_k^T(q^{-1}) = (q - q^{-1})P_k,$$

where P_k is the standard permutation matrix $P_k := \sum_{1 \leq i, j \leq k} e_{ij}^1 \otimes e_{ji}^2$. The total transposition $\mathcal{R}_k^T(q)$ of $\mathcal{R}_k(q)$ results in interchanging the space labels $1 \leftrightarrow 2$.

In Fig. 7 we have an example of a directed network with 6 sources and 12 sinks. Adding additional face weights Z_{n00} , Z_{0n0} , Z_{00n} to the Fock-Goncharov quiver for SL_n we noticed that the dual oriented planar graph G can be redrawn in the rectangle with n sources on the left and $2n$ sinks on the right (check Fig. 7 for $n = 6$ example); then \mathcal{M} has a block matrix form

$\mathcal{M} = \begin{pmatrix} \mathcal{M}_1 \\ \mathcal{M}_2 \end{pmatrix}$ in which we let \mathcal{M}_1 is the upper $n \times n$ block and \mathcal{M}_2 is the lower $n \times n$ block. We want to show that Lemma 7.18 implies the following commutation relations for \mathcal{M}_1 and \mathcal{M}_2 :

$$(2.7) \quad \mathcal{R}_n(q) \overset{1}{\mathcal{M}}_i \otimes \overset{2}{\mathcal{M}}_i = \overset{2}{\mathcal{M}}_i \otimes \overset{1}{\mathcal{M}}_i \mathcal{R}_n(q), \quad i = 1, 2,$$

and

$$(2.8) \quad \overset{1}{\mathcal{M}}_1 \otimes \overset{2}{\mathcal{M}}_2 = \overset{2}{\mathcal{M}}_2 \otimes \overset{1}{\mathcal{M}}_1 \mathcal{R}_n(q).$$

We rewrite the above matrix $\mathcal{R}_{2n}(q)$ as

$$\begin{aligned} \mathcal{R}_{2n}(q) &= \sum_{1 \leq i, j \leq n} e_{ii}^1 \otimes e_{jj}^2 + (q - 1) \sum_{1 \leq i \leq n} e_{ii}^1 \otimes e_{ii}^2 + (q - q^{-1}) \sum_{1 \leq j < i \leq n} e_{ij}^1 \otimes e_{ji}^2 \\ &+ \sum_{1 \leq i, j \leq n} e_{n+i, n+i}^1 \otimes e_{n+j, n+j}^2 + (q - 1) \sum_{1 \leq i \leq n} e_{n+i, n+i}^1 \otimes e_{n+i, n+i}^2 \\ &\quad + (q - q^{-1}) \sum_{1 \leq j < i \leq n} e_{n+i, n+j}^1 \otimes e_{n+j, n+i}^2 \\ &+ \sum_{1 \leq i, j \leq n} e_{i, i}^1 \otimes e_{n+j, n+j}^2 \\ &+ \sum_{1 \leq i, j \leq n} e_{n+i, n+i}^1 \otimes e_{j, j}^2 + (q - q^{-1}) \sum_{1 \leq i, j \leq n} e_{n+i, j}^1 \otimes e_{j, n+i}^2 \end{aligned}$$

In the first two lines we immediately recognize $\mathcal{R}_n(q)$ in two diagonal $n \times n$ blocks of $\mathcal{R}_{2n}(q)$: the relations for the pair of first indices (i, j) and $(n+i, n+j)$ generate (2.7) for \mathcal{M}_1 and \mathcal{M}_2 respectively; setting $(i, n+j)$, which corresponds to the third line, we obtain just a unit matrix in the left-hand side thus producing relation (2.8), whereas in the case $(n+i, j)$ (the fourth line), we have the equation

$$\overset{1}{\mathcal{M}}_2 \otimes \overset{2}{\mathcal{M}}_1 + (q - q^{-1})P_n \overset{1}{\mathcal{M}}_1 \otimes \overset{2}{\mathcal{M}}_2 = \overset{2}{\mathcal{M}}_1 \otimes \overset{1}{\mathcal{M}}_2 \mathcal{R}_n(q).$$

We first push the permutation operator P_n through the \mathcal{M} -matrix product interchanging the labels of spaces in the direct product and then use the identity $(q - q^{-1})P_n = \mathcal{R}_n(q) - \mathcal{R}_n^T(q^{-1})$ obtaining

$$\overset{1}{\mathcal{M}}_2 \otimes \overset{2}{\mathcal{M}}_1 + \overset{2}{\mathcal{M}}_1 \otimes \overset{1}{\mathcal{M}}_2 (\mathcal{R}_n(q) - \mathcal{R}_n^T(q^{-1})) = \overset{2}{\mathcal{M}}_1 \otimes \overset{1}{\mathcal{M}}_2 \mathcal{R}_n(q),$$

or

$$\overset{1}{\mathcal{M}}_2 \otimes \overset{2}{\mathcal{M}}_1 = \overset{2}{\mathcal{M}}_1 \otimes \overset{1}{\mathcal{M}}_2 \mathcal{R}_n^T(q^{-1}),$$

which is just another form of writing relation (2.8). This accomplishes the proof of relations 2.7 and 2.8. \square

Remark 2.4. In [38] the cluster realization of the quantum group $U_q(SL_n)$ was constructed. Combined together with description in the form of planar networks in [39] it implies another proof of formula 2.7.

Now, in order to obtain the commutation relations for normalized transport matrices M_1 and M_2 we have to eliminate extra variables $Z_{n,0,0}$, $Z_{0,n,0}$ and $Z_{0,0,n}$. Henceforth, we normalize the matrices \mathcal{M}_i , $i = 1, 2$ by multiplying them by corresponding monomials. More exactly, we multiply the matrix \mathcal{M}_1 by D_1^{-1} , where D_1 is the function (6.1) commuting with all elements of \mathcal{M}_1 . Clearly, $D_1^{-1}\mathcal{M}_1$ will be independent of Z_{n00} . Similarly, we multiply \mathcal{M}_2 by $\bullet D_1^{-1}D_2^{-1}\bullet$ where $D_2 = \tau^2 D_1$ is the similar monomial that starts with the variable Z_{0n0} . These multiplications preserve the form of relations (2.7) and their only effect on (2.7) is the appearance of the constant factor in the R -matrix in the right-hand side (this is because D_1 commutes with $\bullet D_1^{-1}D_2^{-1}\bullet\mathcal{M}_2$, and $\bullet D_1^{-1}D_2^{-1}\bullet$ commutes with $D_1^{-1}\mathcal{M}_2$; only D_1 and D_2 do not commute).

We now define the *normalized quantum monodromy* or *normalized quantum transport matrices* of the *standard SL_n quiver*:

Definition 2.5. Normalized quantum transport matrices are defined as follows

$$M_1 = QSM_1D_1^{-1} \text{ and } M_2 = QSM_2D_1^{-1}D_2^{-1}$$

where $Q = \text{diag}\{(-q)^{n-i}\}$.

Note that

$${}^1Q \otimes {}^2Q \mathcal{R}_n(q) = \mathcal{R}_n(q) {}^1Q \otimes {}^2Q \text{ for any diagonal matrix } Q$$

and

$${}^1S \otimes {}^2S \mathcal{R}_n(q) = \mathcal{R}_n^T(q) {}^1S \otimes {}^2S \text{ for any antidiagonal matrix } S.$$

We have therefore proved the following theorem.

Theorem 2.6. *The above M_1 and M_2 satisfy the relations*

$$\begin{aligned} R_n^T(q) {}^1M_i \otimes {}^2M_i &= {}^2M_i \otimes {}^1M_i R_n(q) \\ {}^1M_1 \otimes {}^2M_2 &= {}^2M_2 \otimes {}^1M_1 R_n(q) \end{aligned}$$

where

$$(2.9) \quad R_n(q) = q^{-1/n} \left[\sum_{i,j} {}^1e_{ii} \otimes {}^2e_{jj} + (q-1) \sum_i {}^1e_{ii} \otimes {}^2e_{ii} + (q-q^{-1}) \sum_{i>j} {}^1e_{ij} \otimes {}^2e_{ji} \right]$$

is the quantum trigonometric R -matrix

Remark 2.7. G.Schrader and A.Shapiro obtained independently a proof of Theorem 2.6 using the cluster representation of the mapping class group action that will be published elsewhere [40].

Theorem 2.8. *The quantum transport matrices T_i satisfy the quantum groupoid relation*

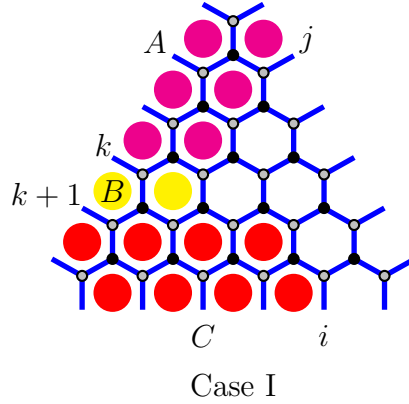
$$T_1T_2T_3 = \text{Id}.$$

Remark 2.9. Recalling $M_1 = T_1$, $M_2 = T_2^{-1}$ we have $T_3M_1 = M_2$.

Proof. The product T_3T_1 is given by the following double sum over directed paths:

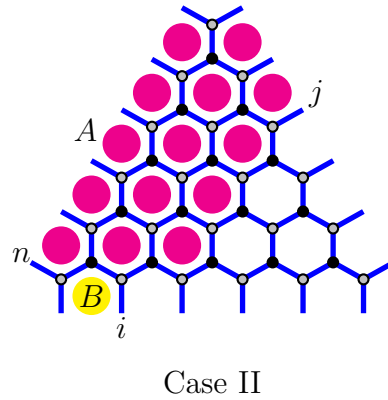
$$(2.10) \quad [(QS)^{-1}T_3T_1]_{ij} = \sum_{k=1}^n (-1)^k q^{n-k} \sum_{\text{paths } k \rightarrow i} : \prod Z_\alpha : \sum_{\text{paths } j \rightarrow k} : \prod Z_\beta : \dots$$

We now consider the pattern in the figure below. We do not indicate arrows on edges recalling that all paths in T_1 go from right to left and from top to bottom whereas all paths in T_3 go from left to right and from top to bottom. Two paths: $j \rightarrow k$ from T_1 and $k \rightarrow i$ from T_3 share the common horizontal leg; if we remove this leg then the remaining part of the union of $j \rightarrow k$ and $k \rightarrow i$ is a path that first goes from right to left, then (in a general Case I) has the leftmost vertical edge, then goes from left to right. In a very special Case II, the path does not have the last part; this happens only for $k = n$ and only if the last horizontal part of the path $j \rightarrow k = n$ is strictly longer than the shared horizontal leg



In Case I, given a path $j \rightarrow k$ encompassing the region A and a path $k \rightarrow i$ encompassing the regions B and C we have the corresponding path $j \rightarrow k + 1$ encompassing the regions A and B and the path $k + 1 \rightarrow i$ encompassing the region C . These pairs of paths are in bijection being the only two possible combinations of paths having the same union of domains $A \cup B \cup C$. Contributions from these two pairs of paths have opposite signs and since $\bullet BC \bullet \bullet A \bullet = q \bullet B \bullet \bullet CA \bullet$ they are mutually canceled in the sum (2.10).

The only pairs of paths ($j \rightarrow k, k \rightarrow i$) that do not have counterparts are those for which the region C is absent (Case II):



In this case, $\bullet B \bullet \bullet A \bullet = \bullet BA \bullet$, k is necessarily equal n , and after removing the common leg, all these pairs of paths are in bijection with single paths going from right to left and encompassing the regions A and B ; note that these paths are exactly paths constituting the matrix M_2 ! So the sum in (2.10) just gives the matrix M_2 (up to the factor QS , which we can now reconstruct). We have therefore proved that $T_3 T_1 = M_2$ □

In Section 7.2 we present another proof of the groupoid property using quantum Grassmannian.

Remark 2.10. The semiclassical limit of Theorem 2.6 statement reads

$$\{M_1 \otimes M_2\} = M_2 \otimes M_1 \left(-\frac{1}{n} I \otimes I + r_n \right)$$

where

$$(2.11) \quad r_n = \sum_i e_{ii}^1 \otimes e_{ii}^2 + 2 \sum_{i>j} e_{ij}^1 \otimes e_{ji}^2$$

is the semiclassical r -matrix. Equivalently,

$$\{[M_1]_{ab}, [M_2]_{cd}\} = -\frac{1}{n} [M_1]_{ab} [M_2]_{cd} + [M_1]_{ad} [M_2]_{cb} \theta(b-d), \quad \theta(x) = \begin{cases} 2, & \text{if } x > 0, \\ 1, & \text{if } x = 0, \\ 0, & \text{if } x < 0. \end{cases}$$

Remark 2.11. Note that for the trigonometric R -matrix (2.9) the quantum relation

$$R_n^T(q) M_i \otimes M_i = M_i \otimes M_i R_n(q)$$

has an equivalent form of writing

$$M_i \otimes M_i R_n^T(q) = R_n(q) M_i \otimes M_i \quad \text{for } i = 1, 2.$$

Both these relations generate the same quantum algebra on elements of the matrices M_1 and M_2 and have the same semiclassical limit

$$\{[M_i]_{ab}, [M_i]_{cd}\} = [M_i]_{ad} [M_i]_{cb} (\theta(b-d) - \theta(a-c)) \quad i = 1, 2, \quad \theta(x) = \begin{cases} 2, & \text{if } x > 0, \\ 1, & \text{if } x = 0, \\ 0, & \text{if } x < 0. \end{cases}$$

Example 2.12. For $n = 3$ direct computations show

$$M_1 \otimes M_2 = M_2 \otimes M_1 R_3(q),$$

where

$$R_3(q) = q^{-1/3} \left(\begin{array}{ccc|ccc|ccc} q & 0 & 0 & 0 & 0 & 0 & 0 & 0 & 0 \\ 0 & 1 & 0 & 0 & 0 & 0 & 0 & 0 & 0 \\ 0 & 0 & 1 & 0 & 0 & 0 & 0 & 0 & 0 \\ \hline 0 & q - q^{-1} & 0 & 1 & 0 & 0 & 0 & 0 & 0 \\ 0 & 0 & 0 & 0 & q & 0 & 0 & 0 & 0 \\ 0 & 0 & 0 & 0 & 0 & 1 & 0 & 0 & 0 \\ \hline 0 & 0 & q - q^{-1} & 0 & 0 & 0 & 1 & 0 & 0 \\ 0 & 0 & 0 & 0 & 0 & q - q^{-1} & 0 & 1 & 0 \\ 0 & 0 & 0 & 0 & 0 & 0 & 0 & 0 & q \end{array} \right)$$

Similarly, for both $i = 1, 2$, we have

$$R_3^T(q) M_i \otimes M_i = M_i \otimes M_i R_3(q)$$

Furthermore, direct computation shows $T_2 T_3 T_1 = \text{Id}$.

3. GOLDMAN BRACKETS AND COMMUTATION RELATIONS BETWEEN TRANSPORT MATRICES

To obtain a full-dimensional (without zero entries) form of transport matrices we define transport matrices along more general paths.

Namely, let $\mathbb{D} = (D, \mathbb{M})$ be a disk D with four marked boundary points $\mathbb{M} = \{A, B, D, C\}$ in clockwise order, $(\Delta ABC, \Delta BCD)$ be a triangulation of D and we also assume clockwise orientation of all triangle sides inside every triangle. The space $\mathcal{X}_{SL_n, \mathbb{D}}$ coincides with the space of quadruple of flags; one flag assigned to each marked point. Each oriented side of triangulation gives a projective basis in \mathbb{C}^N . This allows to define transport matrix for any pair of oriented sides as transition matrix for the pair of corresponding bases; the matrix S acts by changing the orientation of the corresponding side. Let $T_{BC \leftarrow AB}$ be a transport in ΔABC from side AB to BC . Pay attention that the sides are oriented and the order of endpoints in side notation matters. Similarly, $T_{CB \leftarrow DC}$ is a transport matrix in ΔBCD from DC to CB . Note that $T_{DC \leftarrow CB} = T_{CB \leftarrow DC}^{-1}$. Then, we define a transport $T_{DC \leftarrow AB}$ from AB to DC as $T_{DC \leftarrow AB} = T_{DC \leftarrow CB} S T_{BC \leftarrow AB} = T_{CB \leftarrow DC}^{-1} S T_{BC \leftarrow AB}$. Crossing side CD between two triangles add an extra factor $S = T_{CB \leftarrow BC}$ because by our agreement all triangles are oriented counterclockwise that implies the opposite orientation of the common side considered in two neighboring triangles that contain the side. Similarly, $T_{BD \leftarrow AB} = T_{BD \leftarrow CB} S T_{BC \leftarrow AB}$.

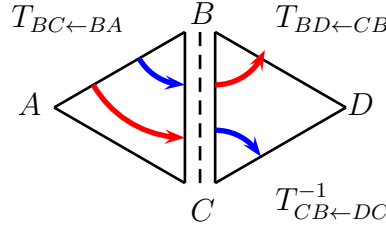
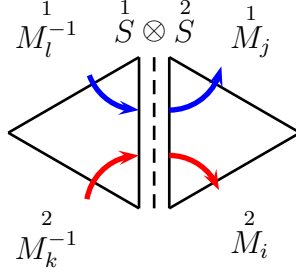


FIGURE 8. Disk with four marked points.

In the quantum case, the cluster variables of triangle ΔABC commute with those of triangle ΔBCD , so the product of two Weyl-ordered monomials is itself a Weyl-ordered monomial, in which we perform an amalgamation of variables on the side BC . Due to the double action of the matrix S , the amalgamation of boundary (frozen) variables in neighbour triangles respects the surface orientation, so, we amalgamate pairwise variables on the sides BC of the two triangles ordered in the same direction, from B to C . After the amalgamation, we unfreeze the obtained new variables. Therefore, for any path along triangles that does not go more than once through any given triangle, the ordering is the Weyl ordering. It was explicitly demonstrated in [39] that the Weyl ordering is preserved by quantum mutations which now include mutations of amalgamated variables as well as mutations of variables in the interior of triangles.

We now show that the commutation relations from Theorem 2.6 together with the groupoid condition (Theorem 2.8) imply the commutativity relations and (semiclassical) Goldman brackets.

We begin with the pattern in the figure below.



We use the identities

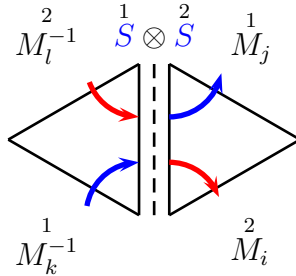
$$\begin{aligned} M_l^{-1} \otimes M_k^{-1} &= R_n(q) M_k^{-1} \otimes M_l^{-1} \\ M_j \otimes M_i &= M_i \otimes M_j R_n^{-T}(q) \\ R_n(q) S^1 \otimes S^2 &= S^1 \otimes S^2 R_n(q)^T \text{ for any antidiagonal matrix } S \end{aligned}$$

We then have

$$\begin{aligned} [M_j^1 S^1 M_l^{-1}] \otimes [M_i^2 S^2 M_k^{-1}] &= M_i^2 \otimes M_j^1 R_n^{-T}(q) S^1 \otimes S^2 R_n(q) M_k^{-1} \otimes M_l^{-1} \\ &= M_i^2 \otimes M_j^1 S^1 \otimes S^2 R_n^{-1}(q) R_n(q) M_k^{-1} \otimes M_l^{-1} = [M_i^2 S^2 M_k^{-1}] \otimes [M_j^1 S^1 M_l^{-1}], \end{aligned}$$

so these two matrix products commute. This is consistent with the quantum mapping class group transformations: flipping BC edge separates the paths $AB \rightarrow BD$ and $AC \rightarrow CD$ into two adjacent triangles.

Consider now the case of two *intersecting* paths (we consider a single intersection inside a quadrangle).



We then have

$$\begin{aligned} [M_j^1 S^1 M_k^{-1}] \otimes [M_i^2 S^2 M_l^{-1}] &= M_i^2 \otimes M_j^1 R_n^{-T}(q) S^1 \otimes S^2 R_n^{-T}(q) M_l^{-1} \otimes M_k^{-1} \\ &= M_i^2 \otimes M_j^1 S^1 \otimes S^2 R_n^{-1}(q) R_n^{-T}(q) M_l^{-1} \otimes M_k^{-1}. \end{aligned}$$

Note that the combination

$$R_n^{-1}(q) R_n^{-T}(q) = q^{2/n} \left[\sum_{i,j} e_{i,i}^1 e_{j,j}^2 + (q^{-2} - 1) \sum_i e_{i,i}^1 e_{i,i}^2 + (q^{-1} - q) \sum_{i \neq j} e_{i,j}^1 e_{j,i}^2 + \sum_{i > j} e_{i,i}^1 e_{j,j}^2 \right]$$

does not admit a nice decomposition itself. However, in the semiclassical limit $q \rightarrow 1$ with $q = e^{\hbar/2}$, it becomes

$$R_n^{-1}(q) R_n^{-T}(q) = I^1 \otimes I^2 + \hbar \left[\frac{1}{n} I^1 \otimes I^2 - P_n \right] + O(\hbar^2),$$

with P_n the permutation matrix, so the term linear in \hbar therefore gives rise to the **Goldman bracket** for SL_n [25].

Let a polygon be triangulated into collection of triangles containing triangle ΔABC , let EF be another side of triangulation different from sides of ΔABC , let γ be a path connecting EF to AB crossing any side of triangulation at most once and crossing neither AC nor BC (see Figure 9). Denote by $T_\gamma = T_{BA \leftarrow EF}$ the composition of transport matrices along the path γ , define transport matrices $M_1 = T_{AB \leftarrow CA}^{-1} S T_\gamma$, $M_2 = T_{BC \leftarrow AB} S T_\gamma$.

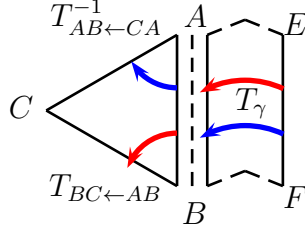


FIGURE 9. $M_1 = T_{CA \leftarrow AB} S T_{BA \leftarrow EF}$, $M_2 = T_{BC \leftarrow AB} S T_{BA \leftarrow EF}$.

Theorem 3.1. *The transport matrices M_1 and M_2 in Fig. 9 satisfy the commutation relations*

$$\begin{aligned} {}^1 M_1 \otimes {}^2 M_2 &= {}^2 M_2 \otimes {}^1 M_1 R_n(q), \\ R_n^T(q) {}^1 M_i \otimes {}^2 M_i &= {}^2 M_i \otimes {}^1 M_i R_n(q) \quad \text{for } i = 1, 2. \end{aligned}$$

and

$$M_2^{-1} M_{BC \leftarrow CA} M_1 = 1.$$

Proof. Consider a transport matrix corresponding to a path not passing twice through the same triangle. It is given by the matrix product $M_{i_{m-1}}^{(m-1)} S \cdots S M_{i_2}^{(2)} S M_{i_1}^{(1)} = T_{BA \leftarrow EF}$ where $i_k = 1, 2$ and variables of $M_{i_k}^{(k)}$ and $M_{i_p}^{(p)}$ commute for distinct k and p . Every such product satisfies the relation $R_n^T(q) \overset{1}{T} \otimes \overset{2}{T} = \overset{2}{T} \otimes \overset{1}{T} R_n(q)$. Then,

$$\begin{aligned} {}^1 M_1^{(m)} \overset{1}{S} \overset{1}{T} \otimes {}^2 M_2^{(m)} \overset{2}{S} \overset{2}{T} &= {}^1 M_1^{(m)} \otimes {}^2 M_2^{(m)} \overset{1}{S} \otimes \overset{2}{S} \overset{1}{T} \otimes \overset{2}{T} = {}^2 M_2^{(m)} \otimes {}^1 M_1^{(m)} R_n(q) \overset{1}{S} \otimes \overset{2}{S} \overset{1}{T} \otimes \overset{2}{T} \\ &= {}^2 M_2^{(m)} \overset{2}{S} \otimes {}^1 M_1^{(m)} \overset{1}{S} R_n^T(q) \overset{1}{T} \otimes \overset{2}{T} = {}^2 M_2^{(m)} \overset{2}{S} \overset{2}{T} \otimes {}^1 M_1^{(m)} \overset{1}{S} \overset{1}{T} R_n(q). \end{aligned}$$

□

General algebras of transport matrices in an ideal triangle decomposition of $\Sigma_{g,s,p}$ —a genus g Riemann surface with s holes and $p > 0$ marked points on the hole boundaries (note that an external edge of an ideal triangle decomposition corresponds to a starting/terminating edge of a path, so we allow only paths starting and terminating at these edges). Transition matrices in this pattern enjoy Fock–Rosly Poisson algebra [20] also considered in [11].

4. REFLECTION EQUATION AND GROUPOID OF UPPER TRIANGULAR MATRICES

4.1. Factorization of an upper-triangular bilinear form \mathbb{A} . We assume again that both M_1 and M_2 are triangular matrices.

The main theorem concerns a special combination of M_1 and M_2 :

$$(4.1) \quad \mathbb{A} := M_1^T M_2.$$

Note that the transposition in the quantum case is formal: the quantum ordering is preserved, only matrix elements are permuted. Also, since M_1 and M_1^T are upper-anti-diagonal matrices and M_2 is a lower-anti-diagonal matrix, the matrix \mathbb{A} is automatically upper-triangular.

Theorem 4.1. *The matrix $\mathbb{A} = M_1^T M_2$ satisfies the quantum reflection equation*

$$R_n(q) \mathbb{A}^1 R_n^{t_1}(q) \mathbb{A}^2 = \mathbb{A}^2 R_n^{t_1}(q) \mathbb{A}^1 R_n(q)$$

with the trigonometric R -matrix (2.9), where $R_n^{t_1}(q)$ is a partially transposed (with respect to the first space) R -matrix.

Proof. The proof is a short direct calculation that uses only R -matrix relations. Note that transposing with respect to the first space the second relation in Theorem 2.6 we obtain

$$M_1^T \otimes M_2 = M_2 R_n^{t_1}(q) M_1^T$$

and the total transposition of the first relation gives

$$R_n(q) M_1^T \otimes M_1^T = M_1^T \otimes M_1^T R_n^T(q),$$

so

$$\begin{aligned} R_n(q) M_1^T M_2 R_n^{t_1}(q) M_1^T M_2 &= R_n(q) M_1^T M_1^T M_2 M_2 = M_1^T M_1^T R_n^T(q) M_2 M_2 \\ &= M_1^T M_1^T M_2 M_2 R_n(q) = M_1^T M_2 R_n^{t_1}(q) M_1^T M_2 R_n(q), \end{aligned}$$

which completes the proof. \square

We thus conclude that **we have a Darboux coordinate representation** for operators satisfying the reflection equation. Moreover *all matrix elements of \mathbb{A} are Laurent polynomials with positive coefficients of Z_α and q* . In particular, positive integers in equation (2.3) count numbers of monomials in the corresponding Laurent polynomials.

By construction of quantum transport matrices in Sec. 2.3, all matrix elements of M_1 and M_2 are Weyl-ordered. For $[\mathbb{A}]_{i,j} = \sum_{k=i}^j [M_1]_{k,i} [M_2]_{k,j}$ we obtain that for $i < j$, $[M_1]_{k,i}$ commutes with $[M_2]_{k,j}$ (all paths contributing to $[M_1]_{k,i}$ are disjoint from all paths contributing to $[M_2]_{k,j}$ for $i < j$), so the corresponding products are also Weyl-ordered, $[\mathbb{A}]_{i,j} = \sum_{k=i}^j \bullet [M_1]_{k,i} [M_2]_{k,j} \bullet$. For $i = j$, the corresponding two paths share the common starting edge, and then $[\mathbb{A}]_{i,i} = q^{-1/2} \bullet [M_1]_{i,i} [M_2]_{i,i} \bullet$. This explains the appearance of $q^{-1/2}$ factors on the diagonal of the quantum matrix \mathbb{A}_n^h (see (1.11), [8]). Note that all Weyl-ordered products of Z_α are self-adjoint and we assume that all Casimirs are also self-adjoint.

To obtain a full-dimensional (not upper-triangular) form of the matrix \mathbb{A} let us consider adjoint action by any transport matrix:

Theorem 4.2. *Any matrix $\mathbb{A}' := M_\gamma^T S^T \mathbb{A} S M_\gamma$ where M_γ is a (transport) matrix satisfying commutation relations of Theorem 2.6 and commuting with $\mathbb{A} = M_1^T M_2$ satisfies the quantum reflection equation of Theorem 4.1.*

The proof is again a direct computation; note also that if we represent $\mathbb{A} = M_1^T M_2$, then $M'_1 = M_1 S M_\gamma$ and $M'_2 = M_2 S M_\gamma$ satisfy commutation relations from Theorem 3.1 and $\mathbb{A}' := M_1'^T M_2'$ then satisfy the quantum reflection equation.

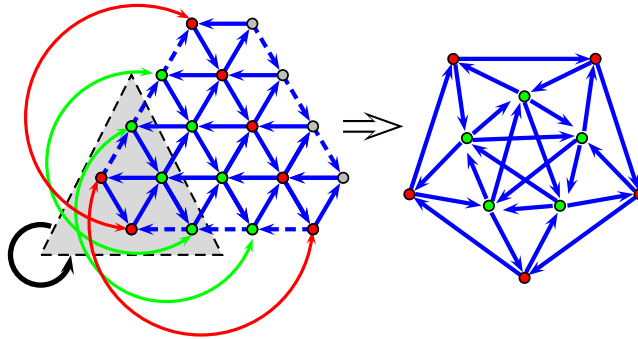
5. THE QUIVER FOR AN UPPER-TRIANGULAR \mathbb{A}_n AND THE BRAID-GROUP ACTION

The goal in this section is, first, to construct the quiver corresponding to the Darboux coordinates of the upper-triangular matrix \mathbb{A}_n and, second, to present the braid-group action on elements of \mathbb{A}_n via chains of mutations in the newly constructed quivers.

5.1. \mathbb{A}_n -quiver. We begin by considering in more details the structure of matrix entries of the product $M_1^T M_2$. Up to inessential numerical factor, we observe that $(M_1^T M_2)_{i,j} \sim \sum_k (\mathcal{M}_1)_{k,i} (\mathcal{M}_2)_{k,j}$ for non-normalized transport matrices (see Definition 7.4), and matrix entries $(\mathcal{M}_1)_{k,i}$ and $(\mathcal{M}_2)_{k,j}$ have coinciding monoidal structures in the respective boundary (frozen) variables $Z_{(k,0,n-k)}$ and $Z_{(n-k,k,0)}$ (see Fig. 6). In the matrix product $M_1^T M_2$ we then have the dependence only on the pairwise products of these variables, which we therefore amalgamate to obtain a single new variable $\bar{Z}_k := \bullet Z_{(k,0,n-k)} Z_{(n-k,k,0)} \bullet$. This results in a “twisted” pattern shown in Fig. 14. Another outcome of this amalgamation procedure is that the resulting quiver admits n new Casimirs depicted in Fig. 15: exactly one such Casimir per every remaining frozen variable $Z_{(0,i,n-i)}$. We can then replace $Z_{(0,i,n-i)}$ by the corresponding commuting product of elements,

$$Z_{(0,i,n-i)} \rightarrow \bullet Z_{(0,i,n-i)}^2 \prod_{j=1}^{i-1} Z_{j,i-j,n-i} \bar{Z}_i \prod_{j=1}^{n-i-1} Z_{j,i,n-i-j} \bullet.$$

Because this product is a Casimir, it becomes an isolated vertex in the obtained quiver. We eventually unfreeze the variables \bar{Z}_k , and then the connected part of the resulting quiver, which we call the \mathbb{A}_n quiver, contains only unfrozen variables. A convenient, and the most symmetric, way of drawing this quiver is to “cut out” the half-sized triangle located in the left-lower corner, then reflect this small triangle through the diagonal passing through its left-lower corner preserving the incidence relations for arrows in the both parts of the quiver, then glue pairwise the amalgamated variables $Z_{(k,0,n-k)}$ and $Z_{(n-k,k,0)}$. Amalgamation operations become planar in this procedure schematically depicted below for \mathbb{A}_5 .



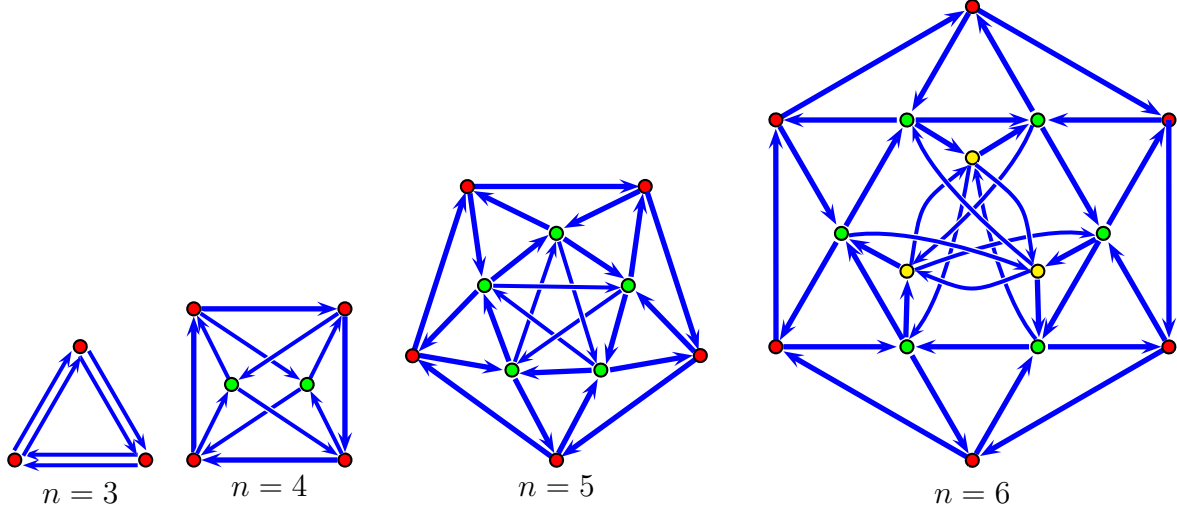
Note that $[n/2]$ original Casimirs give rise to $[n/2]$ Casimir elements

$$C_k = \bullet \bar{Z}_k \prod_{i=1}^{n-k-1} Z_{(k,i,n-k-i)} \bar{Z}_{n-k} \prod_{j=1}^{k-1} Z_{(n-k,j,k-j)} \bullet$$

of the \mathbb{A}_n quiver (vertices of the same color contribute to the same quiver).

We present the resulting quivers for $n = 3, 4, 5, 6$ (they look aesthetically nicer for odd n). In the figure, vertices of the same color enter the same Casimir element and we have $[n/2]$

independent Casimir elements depicted in Fig. 16 in every quiver.



Since all Casimirs of \mathbb{A}_n are generated by λ -power expansion terms for $\det(\mathbb{A}_n + \lambda\mathbb{A}_n^T)$, we automatically obtain the following lemma

Lemma 5.1. $\det(\mathbb{A}_n + \lambda\mathbb{A}_n^T) = P(C_1, \dots, C_{[n/2]})$, where C_i are Casimirs of the \mathbb{A}_n -quiver.

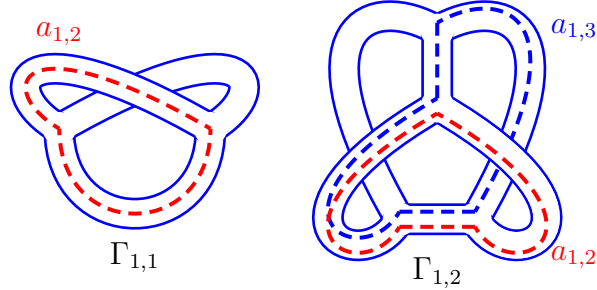
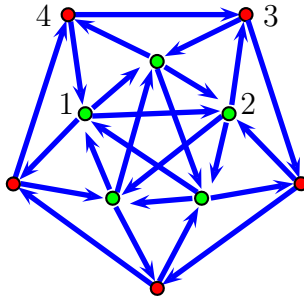


FIGURE 10. Fat graphs $\Gamma_{1,1}$ and $\Gamma_{1,2}$ corresponding to the respective quivers for \mathbb{A}_3 and \mathbb{A}_4 . We indicate closed paths that yield elements $a_{1,2}$ of \mathbb{A}_3 and $a_{1,2}$ and $a_{1,3}$ of \mathbb{A}_4 . For example, setting all $Z_\alpha = 1$, using formulas from [6] for the corresponding geodesic functions we obtain $\text{tr}(LR) = 3$ for $a_{1,2}$ in \mathbb{A}_3 and $\text{tr}(LLR) = 4$ and $\text{tr}(LLRR) = 6$ for the respective $a_{1,2}$ and $a_{1,3}$ in \mathbb{A}_4 , where $L = \begin{bmatrix} 1 & 0 \\ 1 & 1 \end{bmatrix}$ and $R = \begin{bmatrix} 1 & 1 \\ 0 & 1 \end{bmatrix}$ are matrices of respective left and right turns undergoing by paths at three-valent vertices of a spine. It is easy to see that the above values of $a_{i,j}$ coincide with those in Example 2.2.

Remark 5.2. In the cases $n = 3$ and $n = 4$, the constructed quivers are those of geometric systems: these cases admit three-valent fat-graph representations in which Y-cluster variables are identified with (exponentiated) Thurston shear coordinates z_α enumerated by edges of the corresponding graphs, and nontrivial commutation relations are between variables on adjacent edges; for $n = 3$ and $n = 4$ these graphs are the relative spines of Riemann surfaces $\Sigma_{1,1}$ and $\Sigma_{1,2}$ depicted in Fig. 10; the Laurent polynomials for entries of \mathbb{A}_n coincide up to a linear change of log-canonical variables with the expressions obtained by identifying these entries with *geodesic functions* corresponding to closed paths on these graphs; for more details and for the explicit construction of geodesic functions, see [6], [8]. Note here that, likewise all $a_{i,j}$ constructed in this paper, all geodesic functions for all surfaces $\Sigma_{g,s}$ are positive Laurent polynomials of $e^{z_\alpha/2}$.

5.2. Braid-group action through mutations. Our second major goal in this paper is to find a representation of the braid-group action from Sec. 1.3 in terms of cluster mutations of the \mathbb{A}_n -quiver. It is well-known that if we identify $a_{i,j}$ with the geodesics functions, these braid-group transformations correspond to Dehn twists along geodesics corresponding to geodesic functions $a_{i,i+1}$ on $\Sigma_{g,s}$. We know that every Dehn twist on a Riemann surface $\Sigma_{g,s}$ can be presented as a chain of mutations of shear variables on edges of the corresponding spine $\Gamma_{g,s}$. Whereas, for $n = 3$ and $n = 4$, \mathbb{A}_n quivers are geometric, and the corresponding mutation sequences are identical, for larger n quivers become essentially different and we have to start from the scratch. However, knowing the answer for $n = 3$ and 4 helps in guessing the answer for a general n . To confirm our result we used computer experiments. We begin with the example of \mathbb{A}_5 -quiver:



Then the following chain of standard mutations preserves the form of the original quiver with the interchanged vertices 3 and 4: $\beta_{3,4} = \mu_1\mu_2\mu_3\mu_2\mu_1$; here, μ_i is the quiver mutation at vertex i .

Possibly a most explicit way to represent a set of elementary braid-group transformations for a general \mathbb{A}_n quiver is as follows: take another copy of the triangle representing the quiver, reflect it and glue the resulting triangle to the original one along the bottom side of the latter in a way that amalgamated variables on the sides of two triangles match and the colored vertices representing Casimir elements are stretched along straight lines, see Fig. 11. The sequences of mutations corresponding to elementary generating elements $\beta_{i,i+1}$ of the braid groups are indicated in the figure.

6. CASIMIRS

In this section, we derive complete sets of Casimirs for all relevant (sub)varieties of cluster variables related to regular quivers associated to SL_n systems. All proofs are direct calculations and will be omitted.

6.1. The full-rank SL_n quiver.

Lemma 6.1. *The complete set of Casimir operators for the full-rank SL_n quiver consists of $\lfloor \frac{n}{2} \rfloor$ monomials of Fock-Goncharov parameters Z_{abc} depicted in the figure below for the example of SL_6 : numbers at vertices indicate the power with which the corresponding variable comes into the product; all nonnumbered variables have power zero. All Casimirs correspond to closed broken-line paths in the SL_n quiver with reflections at the boundaries (the “frozen” variables at boundaries enter the product with powers two, powers of non-frozen variables can be 0, 1, 2, and 3, and they count how many times the path goes through the corresponding variable. The total Poisson dimension of the full-rank quiver is therefore $\frac{(n+2)(n+1)}{2} - 3 - \lfloor \frac{n}{2} \rfloor$.*

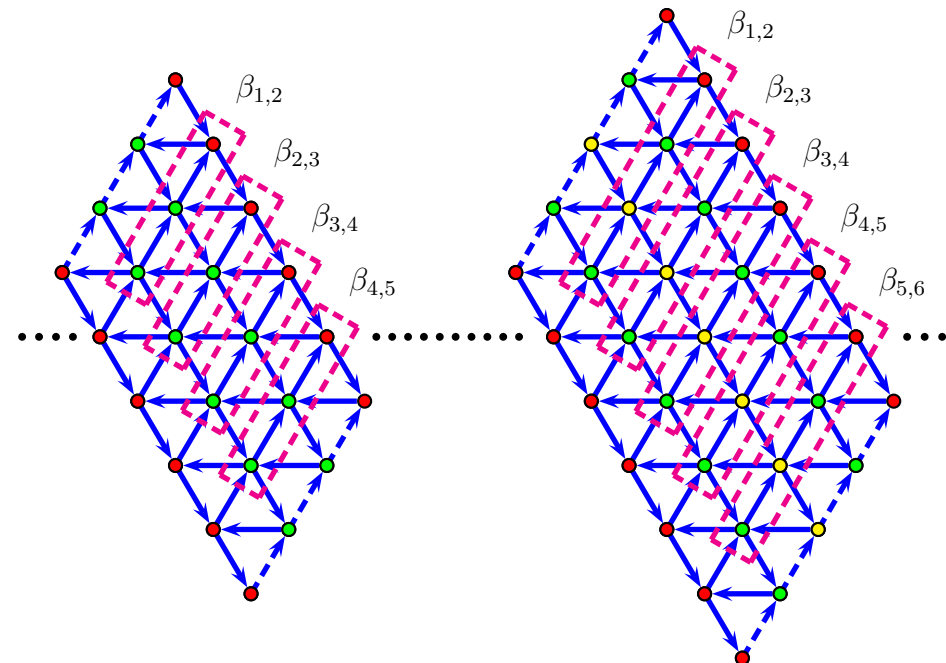


FIGURE 11. Visualising the braid-group action on the union of two triangles, each of which represents the corresponding quiver, for \mathbb{A}_5 and \mathbb{A}_6 . (Note that we can continue this unfolding periodically along the stripes of the same color with the period n .) The dotted line indicates the line of the triangle gluing. Dashed blocks encompass sets of cluster variables sequences of mutations at which produce elementary braid-group transformation $\beta_{i,i+1}$: every such sequence commences with mutating the lowest element inside a box (corresponding to a six-valent vertex), then its upper-right neighbor and so on until we reach the upper element, mutate it, and repeat mutations at all inner elements in the reverse order. So, every such braid-group transformation is produced by a sequence of $2n - 5$ mutations in the quiver corresponding to \mathbb{A}_n .

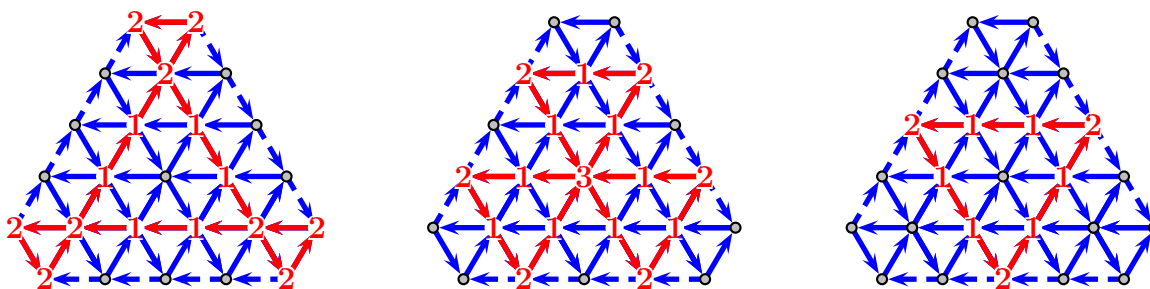


FIGURE 12. Three central elements of the full-rank quiver for SL_6 .

Remark 6.2. All Casimir operators from Lemma 6.1 remain Casimirs for the extended SL_n quiver obtained by adding three more variables Z_{n00} , Z_{0n0} and Z_{00n} at the vertices of the triangle (the variables $Z_{6,0,0}$, $Z_{0,6,0}$, and $Z_{0,0,6}$ in Fig. 17). For the extended SL_n -quiver we have to add one more Casimir operator which is just the product of all frozen variables along all three boundaries of the obtained triangle-shaped quiver.

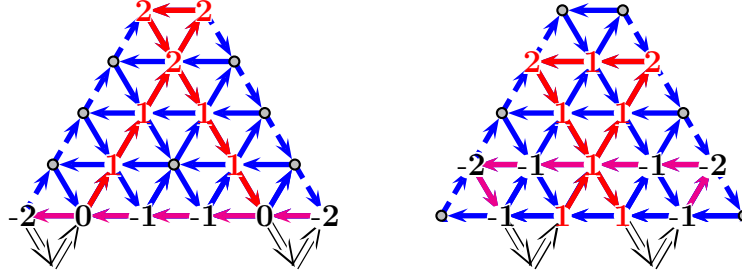


FIGURE 13. Two central elements of the reduced quiver for SL_6 . Every Casimir of the complete quiver in Fig. 12 has its counterpart in the reduced quiver except the third element.

Note that transport matrix M_1 does not depend on the last row of parameters Z_{0bc} , $b+c=n$, while transport matrix M_2 does not depend on the left side Z_{a0c} , $a+c=n$. For completeness, we also present Casimirs for a *reduced quiver* in which we eliminate one of the three sets of frozen variables. In this case, every Casimir of the full-rank quiver has its counterpart in the reduced quiver except the element that is represented by a triangle-shaped path in the full-rank quiver (such an element exists only for even n).

Lemma 6.3. *The complete set of Casimir operators for the reduced SL_n quiver consists of $\lfloor \frac{n-1}{2} \rfloor$ monomials of Fock-Goncharov variables depicted in Fig. 13 for the example of SL_6 : numbers at vertices indicate the power with which the corresponding variable comes into the product; all nonnumbered variables have power zero. All Casimirs correspond, as in Fig. 12, to closed broken-line paths in the corresponding full-rank quiver with reflections at the boundaries (the “frozen” variables at boundaries enter the product with powers two), but now the path is split into two parts separated by two reflections at the side of the triangle that corresponds to the erased frozen variables; these two parts enter with opposite signs; the corresponding Casimir therefore contains cluster variables both in positive and in negative powers. As in the case of full-rank quiver, these powers count (with signs) how many times the path goes through the corresponding variable). The total Poisson dimension of the reduced SL_n quiver is therefore $\frac{n(n+1)}{2} - 1 - \lfloor \frac{n-1}{2} \rfloor$.*

In our construction below, an important role is played by the additional Casimir for the reduced quiver that appears if we add the variable Z_{n00} at the summit of the corresponding triangle. In this case, besides the Casimirs in Lemma 6.3, we have one more central element D_1 :

Lemma 6.4. *The complete set of Casimir operators for the reduced SL_n quiver with the (“frozen”) cluster variable $(0, 0, n)$ added comprises all Casimirs described in Lemma 6.3 plus the element D_1 given by the following formula. The element*

$$(6.1) \quad D_1 = \mathop{\cdot}\prod_{k=1}^n \left[\prod_{i+j=N-k} [Z_{kij}]^{k/n} \right] \mathop{\cdot}$$

is central for the subset of Z_{kij} with $k > 0$. Moreover, the only elements do not commute with D_1 are Z_{00n} and Z_{0n0} . More accurately, $Z_{00n}D_1 = q^{1/n}D_1Z_{00n}$ and $Z_{0n0}D_1 = q^{-1/n}D_1Z_{0n0}$.

6.2. Casimirs for the upper-triangular matrices. Entries of the matrix $\mathbb{A} := M_1^T M_2$ depend on all variables of the SL_n quiver, but due to the transposition, two sets of the frozen variables become amalgamated, that is, only their products appear in the entries of the matrix \mathbb{A} . We explicitly show this amalgamation in Fig. 14.

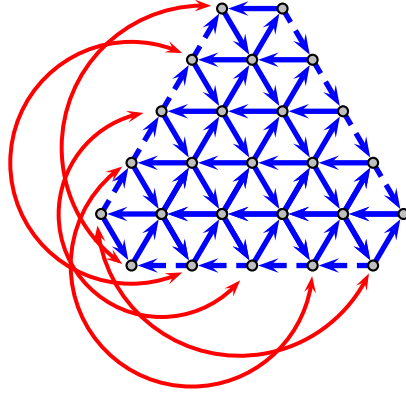


FIGURE 14. The amalgamation of the SL_n -quiver corresponding to the triangle $\Sigma_{0,1,3}$. (The example in the figure corresponds to SL_6 .)

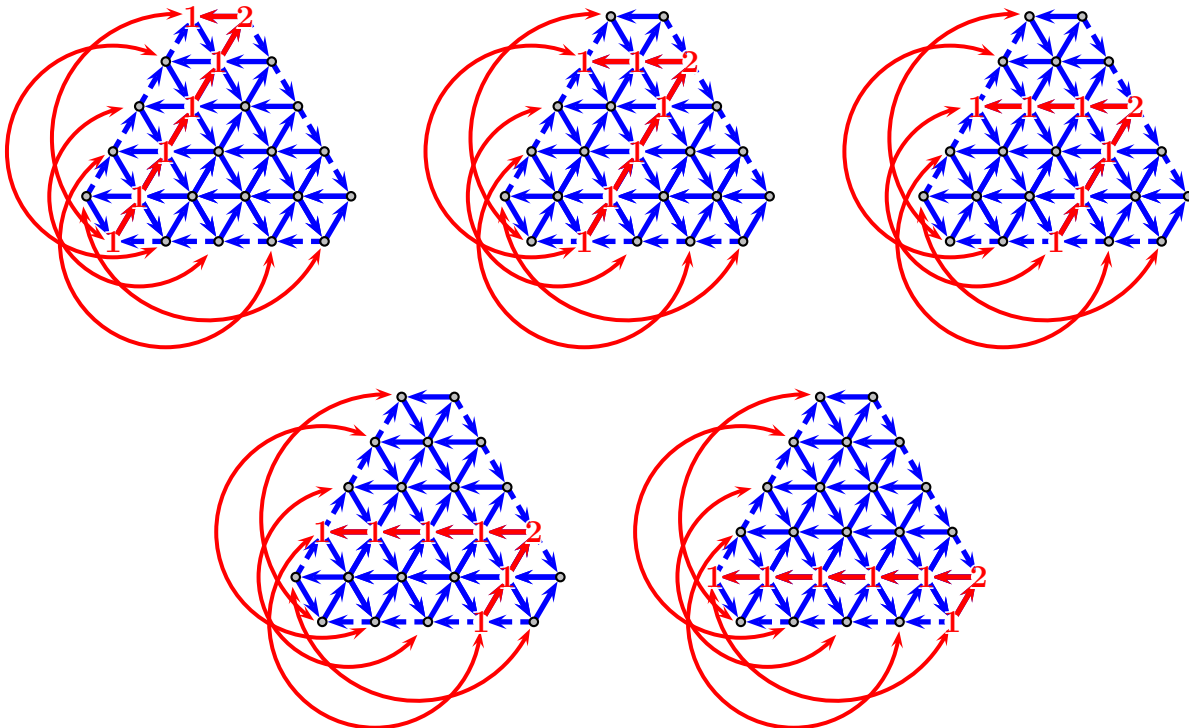


FIGURE 15. Five new central elements of the main quiver for SL_6 due to amalgamation. (These central elements are used to set all diagonal elements of the upper-triangular matrix $\mathbb{A} = M_1^T M_2$ to be the unities.)

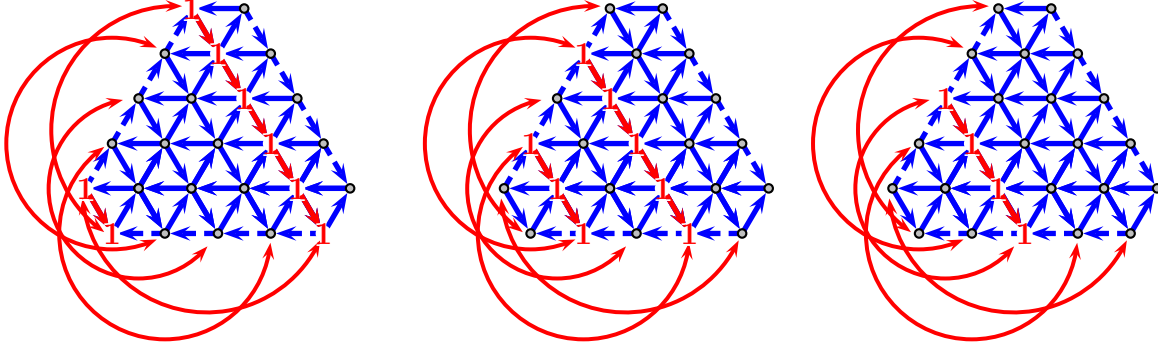


FIGURE 16. Three remaining central elements of the full-rank quiver for SL_6 after amalgamation and setting the diagonal elements of \mathbb{A} equal to unities.

It is easy to see that all Casimirs from Lemma 6.1 remain Casimirs in the amalgamated quiver. We just keep in mind that either four or two frozen variables (depending on the Casimir element) become pairwise amalgamated. More, this amalgamation results in the appearance of $n - 1$ new Casimirs; it is technically more convenient to consider these new Casimirs and some products of them with old Casimirs to obtain a complete set of Casimir operators for the amalgamated quiver.

We use these new Casimirs to eliminate the dependence of \mathbb{A} on remaining $n - 1$ frozen variables: diagonal entries of $\mathbb{A} = M_1^T M_2$ are particular products of these Casimirs, and we adjust the values of these Casimir operators to make all diagonal elements of \mathbb{A} equal to the unities in the classical case and $q^{-1/2}$ in the quantum case (the latter can be justified by assuming the condition that all Casimirs are self-adjoint operators).

Lemma 6.5. *The complete set of central elements for the amalgamated quiver in Fig. 14 comprises $n - 1$ new Casimirs depicted in Fig. 15 for the case of SL_6 and $\lfloor \frac{n}{2} \rfloor$ central elements (products of old Casimirs with the new ones) depicted in Fig. 16.*

7. PROOF OF THEOREM 2.6

In this section we accomplish the proof of Theorem 2.6.

7.1. Normalized and non-normalized transport matrices.

Remark 7.1. An equivalent of the semiclassical limit of Theorem 2.6 (see Remark 2.10) was proved in [24].

To prove the theorem we consider extended Fock-Goncharov quiver with additional vertices labelled $(n00), (0n0)$ and $(00n)$ and construct the oriented dual planar bicolored graph G (Figure 7). Vertices of G are colored into black and white color as follows: a black vertex has two incoming arrows and one outgoing, while a white vertex has two outgoing and one incoming arrows.

Then, we define non-normalized quantum transport matrices \mathcal{M}_1 and \mathcal{M}_2 as quantization of boundary measurement matrices of graph G introduced by Postnikov in [35].

Namely, we assign to every maximal oriented path P connecting a source of G to a sink a quantum weight $w(P)$ in the quantum torus Υ defined by formula 2.4 (see Fig.17).

We define the boundary measurement between source p and sink q as $\mathcal{M}_{pq} = \sum_{\text{path } P:p \rightsquigarrow q} w(P)$.

Noting that G has n sources and $2n$ sinks, we organize boundary measurements \mathcal{M}_{pq} into $2n \times n$

matrix that consists of two $n \times n$ blocks: the top n rows $\mathcal{M}_1 = \mathcal{M}_{[1,n]}$ and the bottom n rows $\mathcal{M}_2 = \mathcal{M}_{[n+1,2n]}$.

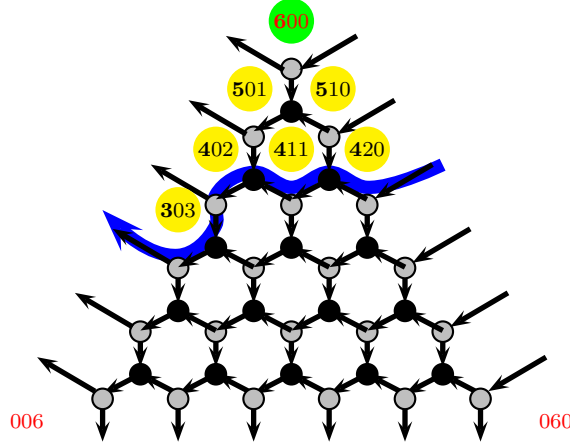


FIGURE 17. Face and path weights of G . Faces are labeled by indices $i, j, k \in \mathbb{Z}$, $i + j + k = 6$, the corresponding Fock-Goncharov face weight is denoted by Z_{ijk} . The weight $w(P)$ of the blue path P is the product of face weights inside colored circles: $w(P) = \bullet Z_{420} Z_{510} Z_{411} Z_{600} Z_{501} Z_{402} Z_{303} \bullet$. Note that faces (600), (060), (006) do not carry Fock-Goncharov variables and don't contribute to the normalized transport matrices M_1 and M_2 . However, they do contribute toward non-normalized transport matrices \mathcal{M}_1 and \mathcal{M}_2 .

Example 7.2. Consider the triangular network of SL_3 (Fig. 18)

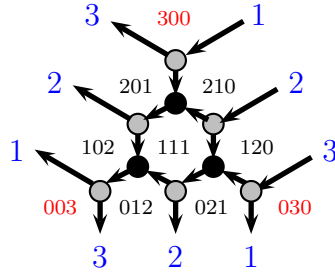


FIGURE 18. Face and path weights of G_{SL_3} . Triples $i, j, k \in \mathbb{Z}$, $i + j + k = 3$ label faces.

Quantum transport matrices have the following form:

$$M_1 = \begin{pmatrix} \bullet Z_{120}^{-1/3} Z_{203}^{1/3} Z_{111}^{-1/3} Z_{210}^{-2/3} Z_{102}^{2/3} \bullet & \bullet Z_{120}^{-1/3} Z_{201}^{1/3} (Z_{111}^{-1/3} + Z_{111}^{2/3}) Z_{201}^{1/3} Z_{102}^{2/3} \bullet & \bullet Z_{120}^{2/3} Z_{201}^{1/3} Z_{111}^{2/3} Z_{210}^{1/3} Z_{102}^{2/3} \bullet \\ \bullet Z_{120}^{-1/3} Z_{201}^{-1/3} Z_{111}^{-1/3} Z_{210}^{-2/3} Z_{102}^{-1/3} \bullet & \bullet Z_{120}^{-1/3} Z_{201}^{-1/3} Z_{111}^{-1/3} Z_{210}^{1/3} Z_{102}^{-1/3} \bullet & 0 \\ \bullet Z_{120}^{-1/3} Z_{201}^{-2/3} Z_{111}^{-1/3} Z_{210}^{-2/3} Z_{102}^{-1/3} \bullet & 0 & 0 \end{pmatrix}.$$

Then, $M_1 = QSD_1^{-1}M_1$, where $D_1 = \bullet Z_{120}^{1/3} Z_{201}^{2/3} Z_{111}^{1/3} Z_{300} Z_{210}^{2/3} Z_{102}^{1/3} \bullet$ and

$$\mathcal{M}_1 = \begin{pmatrix} \bullet Z_{300} \bullet & 0 & 0 \\ \bullet Z_{300} Z_{201} \bullet & \bullet Z_{210} Z_{300} Z_{201} \bullet & 0 \\ \bullet Z_{300} Z_{201} Z_{102} \bullet & \bullet Z_{210} (1 + Z_{111}) Z_{300} Z_{201} Z_{102} \bullet & \bullet Z_{120} Z_{210} Z_{111} Z_{300} Z_{201} Z_{102} \bullet \end{pmatrix}.$$

Fig. 21). For a plabic graph G^{pl} we define an oriented dual graph $(G^{pl})^*$ as follows. Vertices of $(G^{pl})^*$ are faces of G^{pl} . For every black and white vertex x of G^{pl} we define 3 arcs of $(G^{pl})^*$ that cross half-edges attached to x in counterclockwise direction if x is black and clockwise direction if x is white (see Fig. 20).

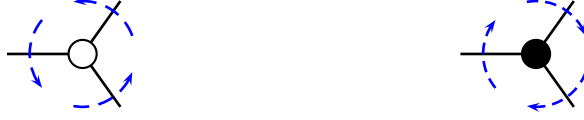


FIGURE 20. Dashed blue arcs are edges of the dual graph $(G^{pl})^*$ around black and white vertex of G^{pl} .

For $\theta, \phi \in \text{Faces}(\mathcal{N})$ let $\#(\theta \rightarrow \phi)$ denote the number of arrows from θ to ϕ in $(G^{pl})^*$. Define the form $\Omega \in (\tilde{V})^* \wedge (\tilde{V})^*$ by the formula

$$(7.2) \quad \Omega(\theta, \phi) = \frac{1}{2} (\#(\theta \rightarrow \phi) - \#(\phi \rightarrow \theta)).$$

Example 7.5. The plabic graph G^{pl} and its dual for the network Fig. 19 are shown on the Fig. 21.

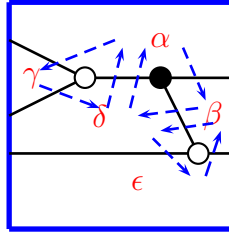


FIGURE 21. Arcs of plabic graph G^{pl} corresponding to network \mathcal{N} on Fig. 19 are black solid lines; arcs of its dual $(G^{pl})^*$ are dashed blue arrows. The form Ω takes following values: $\Omega(\alpha, \beta) = 1/2$, $\Omega(\alpha, \delta) = -1$, $\Omega(\alpha, \gamma) = 1/2$, $\Omega(\beta, \epsilon) = -1/2$, $\Omega(\beta, \delta) = 1$, $\Omega(\gamma, \delta) = 1/2$, $\Omega(\delta, \epsilon) = 1/2$

Let V be the quotient space $V = \tilde{V} / \sum_{\theta \in \text{Faces}(\mathcal{N})} \theta$ and Λ be the integer lattice in V induced by the lattice $\tilde{\Lambda}$ in \tilde{V} . Note that $\sum_{\theta \in \text{Faces}(\mathcal{N})} \theta \in \ker(\Omega)$ and the push forward of Ω to V is well-defined.

Let $a \in \text{Faces}(\mathcal{N})$, Z_a denote its weight. The quantum torus $\Upsilon_{\mathcal{N}}$ is generated by weights Z_a , $a \in \text{Faces}(\mathcal{N})$ satisfying commutation relations $Z_a Z_b = q^{2\Omega(a,b)} Z_b Z_a$. Note that $q^{\Omega(a,b)} Z_a Z_b = q^{\Omega(b,a)} Z_b Z_a$. The Weyl ordering of a monomials in Z_a is defined by $\bullet Z_a Z_b \bullet = q^{\Omega(a,b)} Z_a Z_b$. Evidently, $\bullet Z_a Z_b \bullet = \bullet Z_b Z_a \bullet$. We define weight of any vector in $\Lambda \otimes \mathbb{Q}$ by $Z_{a+b} = \bullet Z_a Z_b \bullet = \bullet Z_b Z_a \bullet$ and $Z_{\lambda a} = \bullet Z_a \bullet^\lambda = \bullet Z_a^\lambda \bullet$ for any $\lambda \in \mathbb{Q}$. Since every Z_a is a positively defined self-adjoint operator in $\ell^2(\mathbb{R})$ having a continuous spectrum $(0, \infty)$, any rational power of it is itself a positively defined self-adjoint operator. Weights satisfy relation $\bullet \prod_{\alpha \in \text{Faces}(\mathcal{N})} Z_\alpha \bullet = 1$, or, equivalently,

$$\sum_{\alpha \in \text{Faces}(\mathcal{N})} \alpha = \mathbf{0} \in V.$$

Let p be the maximal oriented path from a source i on the right to the sink j on the left of a network. Complete the path to the loop $\tilde{p} = g \circ p$ where g is the path around the boundary

of the rectangle going in the clockwise direction from j to i . The oriented loop \tilde{p} defines a covector $\tilde{p} \in \Lambda^*$.

For any $\alpha \in \text{Faces}(N)$ we compute $\tilde{p}(\alpha)$ as follows. Let r be a half infinite ray with starting point inside face α and directed towards infinity and s be an intersection point of r and path \tilde{p} , $T_s r$ be the unit tangent vector to r at s directed in the same direction as r , $T_s \tilde{p}$ is the unit tangent vector to \tilde{p} at s . We assume that r is chosen generic, in the sense that for any intersection point s vectors $T_s r$ and $T_s \tilde{p}$ are linearly independent.

We define the *signed intersection number* $\text{int}_s(\tilde{p}, r)$ of \tilde{p} and r at s to be 1 if orientation of basis $(T_s \tilde{p}, T_s r)$ coincides with counterclockwise orientation of the plane and -1 otherwise. For any point b in rectangle and any ray r starting from b we define $\tilde{p}(\alpha) = \text{ind}(\tilde{p}, r) = \sum_{s_i \in \tilde{p} \cap r} \text{int}_{s_i}(\tilde{p}, r)$ where the sum is taken over all intersection points s_i of \tilde{p} and r . Note that $\tilde{p}(\alpha)$ does not depend on exact position of starting point while the starting point varies inside the same connected component of complement to \tilde{p} . Since any face α lies entirely in some connected component of \tilde{p} we conclude that $\tilde{p}(\alpha)$ is well defined.

Hence, $\tilde{p} \in \tilde{\Lambda}^*$.

Then, we assign to any path p a vector $v_p = \sum_{\alpha \in \text{Faces}(N)} \tilde{p}(\alpha) \alpha \in \Lambda$. Note that the trivial path ϕ has the vector $v_\phi = \sum_{\alpha \in \text{Faces}(N)} \alpha = \mathbf{0} \in V$. In the example in Section 2.3 where any maximal oriented path p is *non-selfintersecting* the vector v_p is the sum of all faces to the right from the path.

Assign to path p its weight $w_p := Z_{v_p}$.

Let S be the set of all sources of net, F be the set of all sinks of the net. Following construction of Postnikov [35], we define for any source $a \in S$ and sink $b \in F$ a quantum boundary measurement $\mathfrak{Meas}^h(a, b) = \sum_{p: a \rightsquigarrow b} (-1)^{\text{cross}(p)} w_p$, where the sum is taken over all oriented paths p from a to b where the *crossing index* $\text{cross}(p)$ is the number of self-crossings of the path p . For the examples of networks in Section 2.3, $\mathfrak{Meas}^h(a, b) = \sum_{p: a \rightsquigarrow b} w_p$.

Let $n = |S|$, $m = |F|$. Define an $m \times n$ matrix \mathfrak{Meas}^h by $(\mathfrak{Meas}^h)_{ba} = (\mathfrak{Meas}^h(a, b))_{a \in S, b \in F}$. Superindex h indicates the quantum version of boundary measurements in contrast to the classical measurements defined in [35].

$$\text{In Example 19, the matrix } \mathfrak{Meas}^h = \begin{pmatrix} Z_{\alpha+\beta} & Z_\alpha \\ Z_{\alpha+\beta+\gamma} & Z_{\alpha+\gamma} \\ Z_{\alpha+\beta+\gamma+\delta} & 0 \end{pmatrix}.$$

Define $(m+n) \times n$ *extended boundary measurement matrix* $\widetilde{\mathfrak{Meas}}^h$ of network \mathcal{N} . Columns of $\widetilde{\mathfrak{Meas}}^h$ are labelled by boundary sources of network; rows are labelled by all boundary vertices.

To describe matrix elements of $\widetilde{\mathfrak{Meas}}^h$ we introduce the *order* $\text{ord}_{\mathcal{N}}(b)$ of boundary vertex b . Namely, let $b \in [1, m+n]$ be the index of boundary vertex in the chosen counterclockwise labelling. Let p be the number of sources among boundary vertices with indices from 1 to $b-1$. The order is defined by the formula $\text{ord}_{\mathcal{N}}(b) = \begin{cases} p, & \text{if } b \text{ is not a source;} \\ p + \frac{1}{2}, & \text{if } b \text{ is a source.} \end{cases}$. Let

$\mathbb{J}(i) \in [1, m+n]$ be the index of i th source, $i \in [1, n]$; $\mathbb{J} : [1, n] \rightarrow [1, m+n]$ is an increasing function.

$$\text{We define } \left(\widetilde{\mathfrak{Meas}}^h \right)_{ji} = \begin{cases} (-1)^{i+\text{ord}_{\mathcal{N}}(j)} q^{\text{ord}_{\mathcal{N}}(j)} \mathfrak{Meas}^h(i, j), & \text{if } j \text{ is not a source;} \\ q^{\text{ord}_{\mathcal{N}}(j)} \delta_{\mathbb{J}(i), j}, & \text{otherwise.} \end{cases}$$

Example 7.6. In Example 19, the matrix $\widetilde{\text{Meas}}^h = \begin{pmatrix} q^{1/2} & 0 \\ 0 & q^{3/2} \\ -q^2 Z_{\alpha+\beta} & q^2 Z_{\alpha} \\ -q^2 Z_{\alpha+\beta+\gamma} & q^2 Z_{\alpha+\gamma} \\ -q^2 Z_{\alpha+\beta+\gamma+\delta} & 0 \end{pmatrix}$.

Remark 7.7. In [35] a boundary measurement map is defined as a map Meas from the space $\text{Net}_{m \times n}$ of networks with n sources and m sinks to $Gr(n, m+n)$. For each $\mathcal{N} \in \text{Net}_{m \times n}$, Postnikov organized boundary measurements $\text{Meas}(i, j)$ from source i to sink j , $i \in [1, n]$, $j \in [1, m]$ into an $(m+n) \times n$ matrix $\widetilde{\text{Meas}}$ which represents $\text{Meas}(\mathcal{N})$. Let's define the diagonal $(m+n) \times (m+n)$ matrix $D^h = \text{diag}(q^{\text{ord}(j)})_{j=1, m+n}$. Then, $\widetilde{\text{Meas}}^h = D^h \widetilde{\text{Meas}}$. We denote by $\text{Mat}_{(m+n) \times n}(\Upsilon_N)$ the space of $(m+n) \times n$ matrices with elements in Υ_N . The group $GL_n(\Upsilon_N)$ of invertible $n \times n$ matrices with entries from Υ_N acts on $\text{Mat}_{(m+n) \times n}(\Upsilon_N)$ by the right multiplication. We define the homogeneous space $Gr^h(n, m+n)$ as the right quotient $Gr^h(n, m+n) = \text{Mat}_{(m+n) \times n}(\Upsilon_N) / GL_n(\Upsilon_N)$. We define the map $\text{Meas}^h : \text{Net}_{m \times n} \rightarrow Gr^h(n, m+n)$ as the composition $\text{Net}_{m \times n}^h \rightarrow \text{Mat}_{(m+n) \times n}(\Upsilon_N) \rightarrow Gr^h(n, m+n)$ which is a quantization of Postnikov measurement map Meas .

Definition 7.8. Two quantum networks \mathcal{N}_1 and \mathcal{N}_2 are *equivalent* if $\text{Meas}^h(\mathcal{N}_1) = \text{Meas}^h(\mathcal{N}_2)$.

Simple equivalence relations (M1-M3, R1-R3) on the space of networks ([35]) are simple local network transformations preserving boundary measurements. Please, note that in the figures below we draw the plabic graph assuming that it is equipped with a perfect orientation. Different choices of compatible perfect orientation give the same result.

The following claims generalize similar statements for commuting weights (cf. [35]).

Let α_0 be the label of one face of oriented planar quiver Γ in the disk attached to the boundary of the disk, $\text{Faces}_0 = \text{Faces} \setminus \{\alpha_0\} = \{\alpha_1, \dots, \alpha_k\}$, $k = |\text{Faces}_0|$. Let $\{\alpha_i | i \in [1, k]\}$ denote the standard basis in the lattice $\Lambda \simeq \mathbb{Z}^k$; for $\mathbf{v}, \mathbf{w} \in \Lambda$ let $\mathbf{v} \cdot \mathbf{w}$ denote the standard dot product $\alpha_i \cdot \alpha_j = \delta_{ij}$, $Z_i = Z_{\alpha_i}$ be the generators of a quantum torus Υ . We say that an infinite linear combination $\sum_{\lambda \in \Lambda} \alpha_\lambda Z_\lambda$ is a Laurent series if there exist integers $b_1, \dots, b_n \in \mathbb{Z}$ such that $\alpha_\lambda = 0$ unless $\lambda \cdot \alpha_j \geq b_j \forall j \in [1, n]$. Any Laurent series $u \in \hat{L}$ where $\hat{L} = \mathbb{Q}[q, q^{-1}][Z_1^{-1}, \dots, Z_k^{-1}][[Z_1, \dots, Z_k]]$. Let $\mathfrak{m} \subset \mathbb{Q}[q, q^{-1}][Z_1, \dots, Z_k]$ be the maximal ideal generated by Z_i . Note that for any $x \in \mathfrak{m}$ the expression $(1+x)^{-1} \in \hat{L}$ and $(1+x^{-1})^{-1} = x(1+x)^{-1} \in \hat{L}$.

We say that $x, y \in \hat{L}$ *q-commute* if $xy = q^r yx$ for some $r \in \mathbb{Q}$.

We call an oriented planar network whose faces are equipped with q -commuting face weights in \hat{L} a *quantum network*.

Define 6 elementary moves (M1-M3), (R1-R3) as shown below.

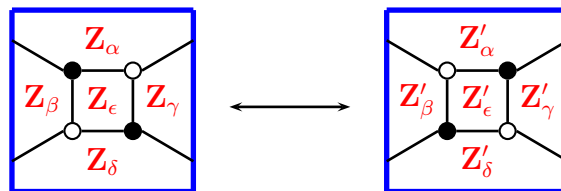


FIGURE 22. Elementary move M1: $Z'_\epsilon = Z_{-\epsilon}$, $Z'_\delta = Z_\delta + Z_{\delta+\epsilon}$, $Z'_\alpha = Z_\alpha + Z_{\alpha+\epsilon}$, $Z'_\beta = \sum_{j=1}^{\infty} (-1)^{j-1} Z_{\beta+j\epsilon}$, $Z'_\gamma = \sum_{j=1}^{\infty} (-1)^{j-1} Z_{\gamma+j\epsilon}$.

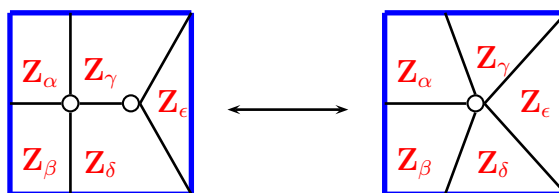


FIGURE 23. Elementary move M2.

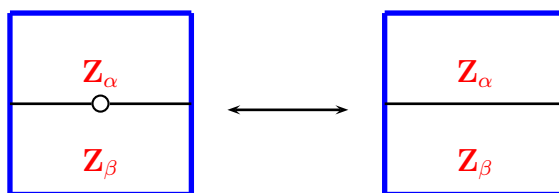


FIGURE 24. Elementary move M3.

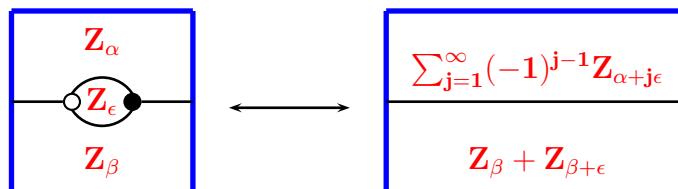


FIGURE 25. Elementary move R1.

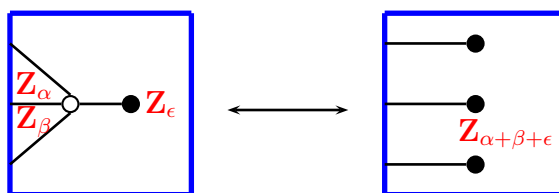


FIGURE 26. Elementary move R2.

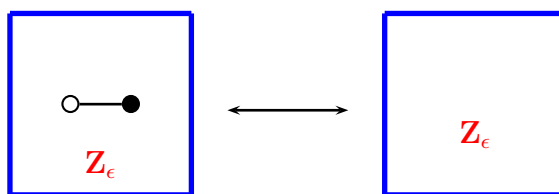


FIGURE 27. Elementary move R3.

Definition 7.9. Two networks are *move equivalent* if they are connected by a sequence of elementary moves.

The corresponding (move) equivalence is called *quantum (move) equivalence*.

The following result extends the results of [35] to quantum networks.

Lemma 7.10. *Two quantum move equivalent networks are quantum equivalent.*

Proof. The proof follows [35]. Compared to the commutative case we just need to check one additional condition that new parameters form q-commutative family. The cases R2,R3, M2, and M3 are evident. Let's consider M1 and R1. The case M1 is proved in [17]. We give the proof here for completeness.

We want to show that $Z'_\alpha, Z'_\beta, Z'_\gamma, Z'_\delta$ and Z'_ϵ q-commute. Indeed,

$$Z'_\alpha Z'_\beta = (Z_\alpha + Z_{\alpha+\epsilon}) \sum_{j=1}^{\infty} (-1)^{j-1} Z_{\beta+j\epsilon} = q^{-\Omega(\alpha,\beta+\epsilon)} Z_{\alpha+\beta+\epsilon};$$

more, $Z'_\beta Z'_\alpha = q^{\Omega(\alpha,\beta+\epsilon)} Z_{\alpha+\beta+\epsilon}$. Therefore, $Z'_\beta Z'_\alpha = q^{2\Omega(\alpha,\beta+\epsilon)} Z'_\alpha Z'_\beta$. All other pairs of parameters can be checked similarly.

Different perfect orientations are in one-to-one correspondence with the *almost perfect matchings* (see [36]). Up to evident symmetries, there are two essentially different perfect orientations. The straightforward computation shows that the elementary move M1 does not change measurements for any choice of perfect orientation.

The case R1 is similar. □

Definition 7.11. ([35]) We say that a plabic network (or graph) is *reduced* if it has no isolated connected components and there is no network/graph in its move-equivalence class to which we can apply a reduction (R1) or (R2). A leafless reduced network/graph is a reduced network/graph without non-boundary leaves.

The following statements are proved in [35] .

Lemma 7.12. [35] *Any network is move equivalent to a reduced network.*

Lemma 7.13. [35] *Two reduced equivalent networks are (M1-M3)-move equivalent.*

Definition 7.14. We call a maximal simple oriented path $P = (p_0, p_1, \dots, p_h)$ ($p_i \neq p_j$ for all $i \neq j$) in a oriented planar network \mathcal{N} *unequivocal* if there is no oriented path $(p_k, q_1, \dots, q_t, p_\ell)$ such that $q_s \neq p_r$ for all $1 \leq s \leq t$ and $0 \leq r \leq h$.

Lemma 7.15. *Let P be an unequivocal path in a oriented planar network $\mathcal{N} \in \text{Net}_{m,n}$. Reversing the orientation of P makes the new oriented planar network \mathcal{N}' which has the same quantum Grassmann measurement $\text{Meas}^h(\mathcal{N}) = \text{Meas}^h(\mathcal{N}')$.*

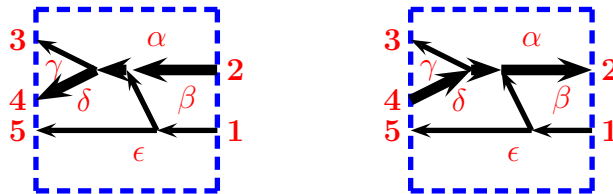


FIGURE 28. Change of orientation of the path $P : 2 \rightsquigarrow 4$

Example 7.16. The corresponding extended quantum measurement matrices are

$$\widetilde{\text{Meas}}^{\hbar} = \begin{pmatrix} q^{1/2} & 0 \\ 0 & q^{3/2} \\ -q^2 Z_{\alpha+\beta} & q^2 Z_{\alpha} \\ -q^2 Z_{\alpha+\beta+\gamma} & q^2 Z_{\alpha+\gamma} \\ -q^2 Z_{\alpha+\beta+\gamma+\delta} & 0 \end{pmatrix} \quad \text{and} \quad (\widetilde{\text{Meas}}^{\hbar})' = \begin{pmatrix} q^{1/2} & 0 \\ qZ_{\beta} & qZ_{\delta+\epsilon+\beta} \\ 0 & qZ_{-\gamma} \\ 0 & q^{3/2} \\ -q^2 Z_{\alpha+\beta+\gamma+\delta} & 0 \end{pmatrix}.$$

Note that $\widetilde{\text{Meas}}^{\hbar} C = (\widetilde{\text{Meas}}^{\hbar})'$, where $C = \begin{pmatrix} 1 & 0 \\ q^{-1/2} Z_{\beta} & q^{-1/2} Z_{\delta+\epsilon+\beta} \end{pmatrix}$.

Indeed, $(\widetilde{\text{Meas}}^{\hbar} C)_{31} = (\widetilde{\text{Meas}}^{\hbar})_{31} + q^{-1/2} (\widetilde{\text{Meas}}^{\hbar})_{32} Z_{\beta} = -q^2 Z_{\alpha+\beta} + q^{3/2} Z_{\alpha} Z_{\beta}$. Recall that $Z_{\alpha} Z_{\beta} = q^{1/2} Z_{\alpha+\beta}$. Therefore, $(\widetilde{\text{Meas}}^{\hbar})_{31} = 0 = ((\widetilde{\text{Meas}}^{\hbar})')_{31}$. Similarly, we can prove equalities for all the entries of these 5×2 matrices and we observe that $\text{Meas}^{\hbar}(\mathcal{N}) = \text{Meas}^{\hbar}(\mathcal{N}') \in \text{Gr}^{\hbar}(2, 5)$.

Proof. Let the simple unequivocal path P in \mathcal{N} goes from a boundary vertex a to a boundary vertex b . We will denote by P^{-1} the path in \mathcal{N}' obtained from P by orientation reversing. We assume first that the boundary vertices are labelled so that $1 \leq a < b \leq m+n$. Since path P is unequivocal there is only one path P from a to b , and $\text{Meas}^{\hbar}(a, b) = w_P$. Moreover, any other path P_1 from s to t where both s and t are distinct from a and b has at most one common interval $[q_1, q_2]$ with path P . The first point q_1 (counting from s) where two paths meet has two incoming arrows and one outgoing and, hence, is colored black, the point q_2 where two paths part is white (see Figure 29). Similarly, any path from a to a sink different from b separates from P at a white point; any path from a sink different from a to b joins path P at a black point.

Recall that $\widetilde{\text{Meas}}^{\hbar}$ is the extended bounded measurement matrix of the network \mathcal{N} , $(\widetilde{\text{Meas}}^{\hbar})'$ is the extended boundary measurement matrix of \mathcal{N}' . Let $F_P \subset \text{Faces}$ denote the subset of all faces to the right of the path P , $v_P = \sum_{\alpha \in F_P} \alpha$. Then, $w_P = Z_{v_P}$, $F_{P^{-1}} = \text{Faces} \setminus F_P$, $v_{P^{-1}} = -v_P$, $w_{P^{-1}} = Z_{v_{P^{-1}}} = Z_{-v_P} = (w_P)^{-1}$.

Consider first the case $1 \leq a < b$.

Let $s < a < t < b$ in the cyclic order of the boundary vertices (see Figure 29). Observe, $w_{b \rightarrow q_1 \rightarrow q_2 \rightarrow t} = Z_{\alpha+\beta+\delta} = \bullet Z_{\beta+\delta} Z_{\alpha} \bullet = \bullet w_{a \rightarrow V \rightarrow W \rightarrow t} \cdot w_{a \rightarrow V \rightarrow W \rightarrow b}^{-1} \bullet = \bullet w_{a \rightarrow q_1 \rightarrow q_2 \rightarrow t} \cdot (\text{Meas}^{\hbar})'_{ab} \bullet$. Since the equality holds for any directed path from b to t , and $\bullet (\text{Meas}^{\hbar})'_{ab} (\text{Meas}^{\hbar})_{ta} \bullet = \bullet (Q_q)_{ta} (\text{Meas}^{\hbar})_{ba}^{-1} \bullet = q^{1/2} (\text{Meas}^{\hbar})_{ta} (\text{Meas}^{\hbar})_{ba}^{-1}$, we conclude that $(\text{Meas}^{\hbar})'_{tb} = \bullet (\text{Meas}^{\hbar})'_{ab} (\text{Meas}^{\hbar})_{ta} \bullet = \bullet (\text{Meas}^{\hbar})_{ba}^{-1} (\text{Meas}^{\hbar})_{ta} \bullet = q^{1/2} (\text{Meas}^{\hbar})_{ta} (\text{Meas}^{\hbar})_{ba}^{-1}$. Similarly, $(\text{Meas}^{\hbar})'_{as} = \bullet (\text{Meas}^{\hbar})'_{ab} (\text{Meas}^{\hbar})_{bs} \bullet = \bullet (\text{Meas}^{\hbar})_{ba}^{-1} (\text{Meas}^{\hbar})_{bs} \bullet = q^{1/2} (\text{Meas}^{\hbar})_{bs} (\text{Meas}^{\hbar})_{ba}^{-1}$ and $(\text{Meas}^{\hbar})_{ts} = \bullet (\text{Meas}^{\hbar})_{bs} (\text{Meas}^{\hbar})'_{tb} \bullet = q^{1/2} (\text{Meas}^{\hbar})_{bs} (\text{Meas}^{\hbar})'_{tb}$. Therefore, $(\text{Meas}^{\hbar})'_{ts} = (\text{Meas}^{\hbar})_{ts} + (\text{Meas}^{\hbar})_{bs} (\text{Meas}^{\hbar})'_{tb} = 0$. Here, $\alpha, \beta, \gamma, \delta$ are appropriate subsets of Faces.

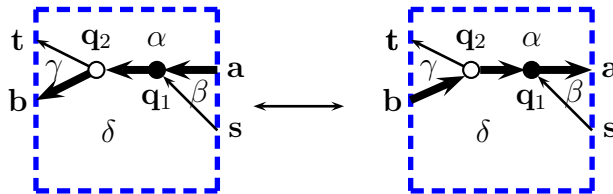


FIGURE 29. Change of the orientation of the path $P : \mathbf{a} \rightsquigarrow \mathbf{b}$, $s < a < t < b$.

In the same way we investigate all the remaining mutual positions of s, t and a, b which leads to the following matrix identity. Let $a_0 = \mathbb{J}^{-1}(a)$, f_0 be the index of source of \mathcal{N} such that b lies between the source f_0 and $f_0 + 1$ (equivalently, $\mathbb{J}(f_0) < b < \mathbb{J}(f_0 + 1)$). Note that $a_0 \leq f_0$ since $a < b$. Define $n \times n$ matrix C for $1 < a < b$ as follows

$$C_{ij} = \begin{cases} \delta_{ij}, & \text{if } i < a_0 \text{ or } i > f_0; \\ q^{-1}\delta_{i-1,j}, & \text{if } a_0 < i \leq f_0 : \\ (-1)^{\lfloor |j-a_0+1/2| \rfloor} q^{-1/2} (\mathcal{M}\text{eas}^h)_{ja} (\mathcal{M}\text{eas}^h)_{ba}^{-1} & \text{if } i = a_0. \end{cases}$$

Then, $(\widetilde{\mathcal{M}\text{eas}^h})' = \widetilde{\mathcal{M}\text{eas}^h} C$.

Note that $(\mathcal{M}\text{eas}^h)' = \mathcal{M}\text{eas}^h C$ implies $\widetilde{\mathcal{M}\text{eas}^h} = (\widetilde{\mathcal{M}\text{eas}^h})' C^{-1}$ where C^{-1} is obtained from C by changing the signs of the off-diagonal elements and adjusting the powers of q . More exactly, define $n \times n$ matrix \widetilde{C} for $1 < b < a$ as follows

$$\widetilde{C}_{ij} = \begin{cases} \delta_{ij}, & \text{if } i \leq f_0 \text{ or } i > a_0; \\ q\delta_{i+1,j}, & \text{if } f_0 < i < a_0 : \\ (-1)^{\lfloor |j-a_0-1/2| \rfloor} q^{1/2} (\mathcal{M}\text{eas}^h)_{ja} (\mathcal{M}\text{eas}^h)_{ba}^{-1} & \text{if } i = a_0. \end{cases}$$

The formulas above induce the same matrix identity $(\widetilde{\mathcal{M}\text{eas}^h})' = \widetilde{\mathcal{M}\text{eas}^h} C$.
These matrix identities prove the statement. \square

Example 7.17. Consider the networks in Figure 30.

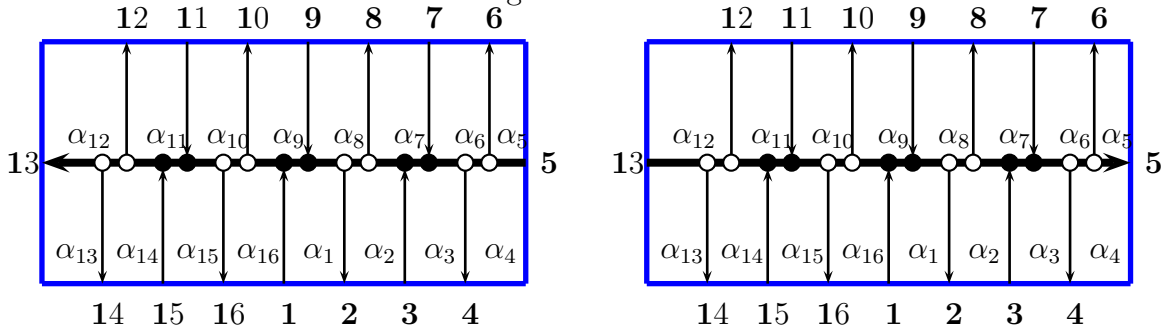


FIGURE 30. Change of the orientation of the unequivocal path $P : 5 \rightsquigarrow 13$, $1 < 5 < 13$.

Matrices $\widetilde{\mathcal{M}\text{eas}^h}$ and $(\widetilde{\mathcal{M}\text{eas}^h})'$ have the following form.

$$\widetilde{\mathcal{M}\text{eas}^h} = \begin{pmatrix} q^{1/2} & 0 & 0 & 0 & 0 & 0 & 0 & 0 \\ 0 & qZ_{-\alpha_2} & -qZ_{-\sum_{j=2}^4 \alpha_j} & qZ_{-\sum_{j=2}^6 \alpha_j} & 0 & 0 & 0 & 0 \\ 0 & q^{3/2} & 0 & 0 & 0 & 0 & 0 & 0 \\ 0 & 0 & q^2 Z_{-\alpha_4} & 0 & 0 & 0 & 0 & 0 \\ 0 & 0 & q^{5/2} & 0 & 0 & 0 & 0 & 0 \\ 0 & 0 & q^3 Z_{\alpha_6} & 0 & 0 & 0 & 0 & 0 \\ 0 & 0 & 0 & q^{7/2} & 0 & 0 & 0 & 0 \\ 0 & q^4 Z_{\sum_{j=3}^7 \alpha_j} & -q^4 Z_{\sum_{j=5}^7 \alpha_j} & q^4 Z_{\alpha_7} & 0 & 0 & 0 & 0 \\ 0 & 0 & 0 & 0 & q^{9/2} & 0 & 0 & 0 \\ q^5 Z_{\sum_{j=1}^9 \alpha_j} & -q^5 Z_{\sum_{j=3}^9 \alpha_j} & q^5 Z_{\sum_{j=5}^9 \alpha_j} & -q^5 Z_{\sum_{j=7}^9 \alpha_j} & q^5 Z_{\alpha_9} & 0 & 0 & 0 \\ 0 & 0 & 0 & 0 & 0 & q^{11/2} & 0 & 0 \\ -q^6 Z_{\sum_{j=1}^{11} \alpha_j} & q^6 Z_{\sum_{j=3}^{11} \alpha_j} & -q^6 Z_{\sum_{j=5}^{11} \alpha_j} & q^6 Z_{\sum_{j=7}^{11} \alpha_j} & -q^6 Z_{\sum_{j=9}^{11} \alpha_j} & q^6 Z_{\alpha_{11}} & -q^6 Z_{-\sum_{j=12}^{14} \alpha_j} & 0 \\ -q^7 Z_{\sum_{j=1}^{12} \alpha_j} & q^7 Z_{\sum_{j=3}^{12} \alpha_j} & -q^7 Z_{\sum_{j=5}^{12} \alpha_j} & q^7 Z_{\sum_{j=7}^{12} \alpha_j} & -q^7 Z_{\sum_{j=9}^{12} \alpha_j} & q^7 Z_{\sum_{j=11}^{12} \alpha_j} & -q^7 Z_{-\sum_{j=13}^{14} \alpha_j} & 0 \\ -q^8 Z_{\sum_{j=1}^{13} \alpha_j} & q^8 Z_{\sum_{j=3}^{13} \alpha_j} & -q^8 Z_{\sum_{j=5}^{13} \alpha_j} & q^8 Z_{\sum_{j=7}^{13} \alpha_j} & -q^8 Z_{\sum_{j=9}^{13} \alpha_j} & q^8 Z_{\sum_{j=11}^{13} \alpha_j} & -q^8 Z_{-\alpha_{14}} & 0 \\ 0 & 0 & 0 & 0 & 0 & 0 & q^{17/2} & 0 \\ q^9 Z_{\sum_{j=1}^{15} \alpha_j} & -q^9 Z_{\sum_{j=3}^{15} \alpha_j} & q^9 Z_{\sum_{j=5}^{15} \alpha_j} & -q^9 Z_{\sum_{j=7}^{15} \alpha_j} & q^9 Z_{\sum_{j=9}^{15} \alpha_j} & 0 & 0 & 0 \end{pmatrix}$$

$$\widetilde{(\mathcal{M}eas^h)'} = \begin{pmatrix} q^{\frac{1}{2}} & 0 & 0 & 0 & 0 & 0 & 0 \\ qZ_{\alpha_1} & 0 & 0 & -qZ_{-\sum_{j=2}^8 \alpha_j} & qZ_{-\sum_{j=2}^{10} \alpha_j} & -qZ_{-\sum_{j=2}^{12} \alpha_j} & qZ_{-\sum_{j=2}^{14} \alpha_j} \\ 0 & q^{\frac{3}{2}} & 0 & 0 & 0 & 0 & 0 \\ -q^2 Z_{\sum_{j=1}^3 \alpha_j} & q^2 Z_{\alpha_3} & q^2 Z_{-\sum_{j=4}^6 \alpha_j} & -q^2 Z_{-\sum_{j=4}^8 \alpha_j} & q^2 Z_{-\sum_{j=4}^{10} \alpha_j} & -q^2 Z_{-\sum_{j=4}^{12} \alpha_j} & q^2 Z_{-\sum_{j=4}^{14} \alpha_j} \\ -q^3 Z_{\sum_{j=1}^4 \alpha_j} & q^3 Z_{\sum_{j=3}^4 \alpha_j} & q^3 Z_{-\sum_{j=5}^6 \alpha_j} & -q^3 Z_{-\sum_{j=5}^8 \alpha_j} & q^3 Z_{-\sum_{j=5}^{10} \alpha_j} & -q^3 Z_{-\sum_{j=5}^{12} \alpha_j} & q^3 Z_{-\sum_{j=5}^{14} \alpha_j} \\ -q^4 Z_{\sum_{j=1}^5 \alpha_j} & q^4 Z_{\sum_{j=3}^5 \alpha_j} & q^4 Z_{-\alpha_6} & -q^4 Z_{-\sum_{j=6}^8 \alpha_j} & q^4 Z_{-\sum_{j=6}^{10} \alpha_j} & -q^4 Z_{-\sum_{j=6}^{12} \alpha_j} & q^4 Z_{-\sum_{j=6}^{14} \alpha_j} \\ 0 & 0 & q^{9/2} & 0 & 0 & 0 & 0 \\ q^5 Z_{\sum_{j=1}^7 \alpha_j} & 0 & 0 & q^5 Z_{-\alpha_8} & -q^5 Z_{-\sum_{j=8}^{10} \alpha_j} & q^5 Z_{-\sum_{j=8}^{12} \alpha_j} & -q^5 Z_{-\sum_{j=8}^{14} \alpha_j} \\ 0 & 0 & 0 & q^{11/2} & 0 & 0 & 0 \\ 0 & 0 & 0 & 0 & q^6 Z_{-\alpha_{10}} & -q^6 Z_{-\sum_{j=10}^{12} \alpha_j} & q^6 Z_{-\sum_{j=10}^{14} \alpha_j} \\ 0 & 0 & 0 & 0 & q^{13/2} & 0 & 0 \\ 0 & 0 & 0 & 0 & 0 & q^7 Z_{-\alpha_{12}} & 0 \\ 0 & 0 & 0 & 0 & 0 & q^{15/2} & 0 \\ 0 & 0 & 0 & 0 & 0 & q^8 Z_{\alpha_{13}} & 0 \\ 0 & 0 & 0 & 0 & 0 & 0 & q^{17/2} \\ 0 & 0 & 0 & 0 & q^9 Z_{\sum_{j=11}^{15} \alpha_j} & -q^9 Z_{\sum_{j=13}^{15} \alpha_j} & q^9 Z_{\alpha_{15}} \end{pmatrix}$$

$$C = \begin{pmatrix} 1 & 0 & 0 & 0 & 0 & 0 & 0 \\ 0 & 1 & 0 & 0 & 0 & 0 & 0 \\ -q^{\frac{1}{2}} Z_{\sum_{j=1}^4 \alpha_j} & q^{\frac{1}{2}} Z_{\sum_{j=3}^4 \alpha_j} & q^{\frac{1}{2}} Z_{-\sum_{j=5}^6 \alpha_j} & -q^{\frac{1}{2}} Z_{-\sum_{j=5}^8 \alpha_j} & q^{\frac{1}{2}} Z_{-\sum_{j=5}^{10} \alpha_j} & -q^{\frac{1}{2}} Z_{-\sum_{j=5}^{12} \alpha_j} & q^{\frac{1}{2}} Z_{-\sum_{j=5}^{14} \alpha_j} \\ 0 & 0 & q & 0 & 0 & 0 & 0 \\ 0 & 0 & 0 & q & 0 & 0 & 0 \\ 0 & 0 & 0 & 0 & q & 0 & 0 \\ 0 & 0 & 0 & 0 & 0 & 0 & 1 \end{pmatrix}$$

It is straightforward to check that $\widetilde{(\mathcal{M}eas^h)'} = \widetilde{\mathcal{M}eas^h} C$.

Consider the network for SL_n shown for $n = 6$ in Figure 17. Let $\Xi = \text{diag}(-1^{n-1}, (-1)^{n-2}, \dots, 1)$.

The boundary measurement matrix $\widetilde{\mathcal{M}eas^h}$ has size $3n \times n$. It consists of three $n \times n$ blocks on top of each other. The top $n \times n$ block $(\widetilde{\mathcal{M}eas^h})_{[1,n]}$ is the diagonal matrix with j th diagonal elements $q^{j-1/2}$. The middle block $(\widetilde{\mathcal{M}eas^h})_{[n+1,2n]}$ is a scalar multiple of the transport matrix $q^n T_2^{-1} \Xi$ and the bottom block $(\widetilde{\mathcal{M}eas^h})_{[2n+1,3n]}$ is a scalar multiple of the transport matrix $q^n T_1 \Xi$ for the network 17.

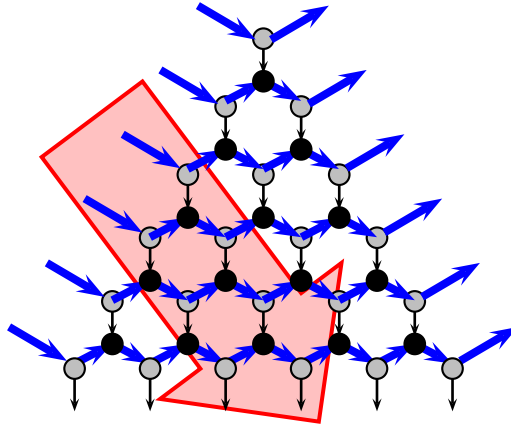


FIGURE 31. Changing orientation of the bold paths. The big arrow shows the direction of transport matrix T_3 .

The orientation change of all blue paths (see Figure 31) leads to the new Grassmann measurement $\widetilde{(\mathcal{M}eas^h)'$. The submatrix $(\widetilde{\mathcal{M}eas^h})'_{[n+1,2n]}$ is a scalar multiple of $T_3 \Xi$. Comparing

blocks $(\widetilde{\mathfrak{Meas}}^h)'_{[n+1,2n]}$ and $(\widetilde{\mathfrak{Meas}}^h)_{[n+1,2n]}$ we obtain $T_2^{-1}T_1^{-1} = T_3$. This is clearly equivalent to the second part of Theorem 3.1: $T_1T_2T_3 = 1$. \square

Commutation relations between face weights induce R -matrix commutation relations between entries of \mathfrak{Meas}^h .

Namely, the next lemma describes the commutation relation between elements of \mathfrak{Meas}^h .

Lemma 7.18. $R_m \overset{1}{\mathfrak{Meas}}^h \otimes \overset{2}{\mathfrak{Meas}}^h = \overset{2}{\mathfrak{Meas}}^h \otimes \overset{1}{\mathfrak{Meas}}^h R_n$, where R_m, R_n are given by formula 2.5.

Proof. We will prove this statement using factorization of matrix \mathfrak{Meas}^h into a product of elementary matrices. Let \mathcal{N} be a network in rectangle with m sinks on the left and n sources on the right all whose arrows are directed right to left. Then, clearly, \mathcal{N} can be presented as a concatenation of elementary networks of two special kinds (see Fig. 32 and 33).

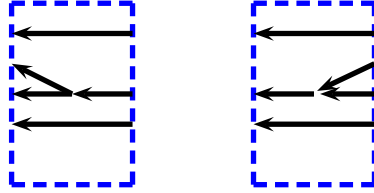


FIGURE 32. Elementary forks (decreasing on the left and increasing on the right)

Figure 33 shows concatenation of a fork.

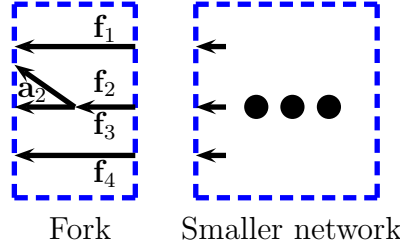


FIGURE 33. Adding fork to the second sink. Note, $\bullet Z_{a_2} Z_{f_1} Z_{f_2} \dots Z_{f_4} \bullet = 1$.

Using the construction above, we write that, $\mathfrak{Meas}^h = \prod_i X_i$, where $X_i = L_i$ or $X_i = U_i$ is an $m_i \times m_{i+1}$ matrix where ($m_{i+1} = m_i - 1$ if we add the decreasing fork or $m_{i+1} = m_i + 1$ if increasing.)

$$L_i = \begin{pmatrix} t_1 & 0 & \dots & \dots & 0 & 0 & \dots \\ 0 & t_2 & \dots & \dots & 0 & 0 & \dots \\ \vdots & & \ddots & & 0 & 0 & \dots \\ \hline 0 & \dots & t_i & 0 & 0 & 0 & \dots \\ 0 & \dots & \bullet t_i Z_{a_i} \bullet & 0 & 0 & 0 & \dots \\ \hline 0 & \dots & 0 & t_{i+1} & 0 & 0 & \dots \\ \dots & & & & & & \ddots \end{pmatrix}, \quad t_1 = \bullet Z_{f_1} \bullet, t_2 = \bullet Z_{f_1} Z_{f_2} \bullet, \text{ etc}$$

and

$$U_i = \begin{pmatrix} t_1 & 0 & \dots & \dots & 0 & 0 & \dots \\ 0 & t_2 & \dots & \dots & 0 & 0 & \dots \\ \vdots & & \ddots & & 0 & 0 & \dots \\ \hline 0 & \dots & \bullet t_i \bullet & \bullet t_i Z_{a_i} \bullet & 0 & \dots \\ \hline 0 & \dots & 0 & 0 & t_{i+1} & \dots \\ & & \dots & & & \ddots \end{pmatrix}, \quad t_1 = \bullet Z_{f_1} \bullet, t_2 = \bullet Z_{f_1} Z_{f_2} \bullet, \text{ etc.}$$

Variables t_j commute with each other and commute with Z_{a_i} unless $j = i$. Otherwise, $Z_{a_i} t_i = q t_i Z_{a_i}$, $\bullet Z_{a_i} t_i \bullet = q^{-1/2} Z_{a_i} t_i$. All entries of X_i commute with all entries of X_j for $i \neq j$.

Clearly, it is enough to check the relations for 2×1 and 1×2 matrices.

For $m_i = 1$, we have $R_{m_i} \overset{1}{L}_i \otimes \overset{2}{L}_i = \overset{2}{L}_i \otimes \overset{1}{L}_i R_{m_{i+1}}$, $R_{m_i} \overset{1}{U}_i \otimes \overset{2}{U}_i = \overset{2}{U}_i \otimes \overset{1}{U}_i R_{m_{i+1}}$. Indeed,

$$\begin{aligned} \begin{pmatrix} q & 0 & 0 & 0 \\ 0 & 1 & 0 & 0 \\ 0 & q - q^{-1} & 1 & 0 \\ 0 & 0 & 0 & q \end{pmatrix} \left[\begin{pmatrix} 1 \\ a \\ b \end{pmatrix} \otimes \begin{pmatrix} 2 \\ a \\ b \end{pmatrix} \right] &= \begin{pmatrix} q & 0 & 0 & 0 \\ 0 & 1 & 0 & 0 \\ 0 & q - q^{-1} & 1 & 0 \\ 0 & 0 & 0 & q \end{pmatrix} \begin{pmatrix} a^2 \\ ab \\ ba \\ b^2 \end{pmatrix} = \\ &= \begin{pmatrix} qa^2 \\ qba \\ qab \\ qb^2 \end{pmatrix} = \left[\begin{pmatrix} 2 \\ a \\ b \end{pmatrix} \otimes \begin{pmatrix} 1 \\ a \\ b \end{pmatrix} \right] \cdot (q) \end{aligned}$$

Then, $R_{m_1} \overset{1}{\mathcal{M}}eas^h \otimes \overset{2}{\mathcal{M}}eas^h = R_{m_1} \prod_{i=1}^n \overset{1}{X}_i \otimes \prod_{i=1}^n \overset{2}{X}_i = R_{m_1} \overset{1}{X}_1 \prod_{i=2}^n \overset{1}{X}_i \otimes \overset{2}{X}_1 \prod_{i=2}^n \overset{2}{X}_i = \overset{2}{X}_1 \otimes \overset{1}{X}_1 R_{m_2} \prod_{i=2}^n \overset{1}{X}_i \otimes \prod_{i=2}^n \overset{2}{X}_i = \dots = \prod_{i=1}^n \overset{1}{X}_i \otimes \prod_{i=1}^n \overset{2}{X}_i R_{m_n} = \overset{1}{\mathcal{M}}eas^h \otimes \overset{2}{\mathcal{M}}eas^h R_{m_n}$. \square

8. CONCLUDING REMARKS

In this paper, we have found the Darboux coordinate representation for matrices \mathbb{A} enjoying the quantum reflection equation. We have also solved the problem of representing the braid-group action for the upper-triangular \mathbb{A} in terms of mutations of cluster variables associated with the corresponding quiver.

In conclusion, we indicate some directions of development. The first interesting problem is to construct mutation realizations for braid-group and Serre element actions that are Poisson automorphisms in the case of block-upper triangular matrices \mathbb{A} (the corresponding action in terms of entries of a block-upper-triangular \mathbb{A} was constructed in [9]). It is not difficult to construct planar networks producing block-triangular transport matrices M_1 and M_2 enjoying the standard Lie Poisson algebra, then $\mathbb{A} = M_1^T M_2$ will satisfy the semiclassical reflection equation.

The second direction of development is based on the semiclassical groupoid construction; explicit calculations in Sec.12 of [10] show that, given that B is a general SL_n -matrix endowed with the standard semiclassical Lie Poisson bracket, solving the matrix equation $B\mathbb{A}B^T = \mathbb{A}'$, where \mathbb{A} and \mathbb{A}' are unipotent upper-triangular matrices, we obtain that entries of \mathbb{A} are uniquely determined (provided all upper-right and lower-left minors of B are nonzero); the Lie Poisson bracket on B produces the reflection equation bracket on \mathbb{A} , the mapping $\mathbb{A} \rightarrow \mathbb{A}'$ is a Poisson anti-automorphism, and finally, entries of \mathbb{A} and \mathbb{A}' are mutually Poisson commute. Therefore, having a set X_α of Darboux coordinates for entries of B we automatically obtain that $a_{i,j} \in \mathbb{Z}[[e^{X_\alpha}]]$ (the determinant of the linear system determining $a_{i,j}$ is the product of central

elements of the Lie Poisson algebra for B). We therefore obtain a hypothetically alternative Darboux coordinate representation, this time for admissible pairs (B, \mathbb{A}) .

ACKNOWLEDGEMENTS

The authors are grateful to Alexander Shapiro for many useful discussion. Our research was supported RFBR Grant No. 18-01-00273 (L.Ch). and NSF research grant DMS #1702115 (M. S.). While working on this project, we benefited from support of the following institutions and programs: Research Institute for Mathematical Sciences, Kyoto (M. S., Spring 2019), Research in Pairs Program at the Mathematisches Forschungsinstitut Oberwolfach (M. S., Summer 2019), and Mathematical Science Research Institute, Berkeley (M. S., Fall 2019). We are grateful to all these institutions for their hospitality and outstanding working conditions they provided.

REFERENCES

- [1] A. Berenstein and A. Zelevinsky, *Quantum cluster algebras* *Advances Math.* **195** (2005) 405–455; math/0404446.
- [2] P. P. Boalch, *Stokes Matrices, Poisson Lie Groups and Frobenius Manifolds*, *Invent. Math.* **146** (3) (2001) 479–506. doi:10.1007/s002220100170.
- [3] A. Bondal, *A symplectic groupoid of triangular bilinear forms and the braid groups*, preprint IHES/M/00/02 (Jan. 2000).
- [4] V. Chari and A. Pressley, *A Guide to Quantum Groups*. Cambridge University Press, 1994.
- [5] Chekhov L., Fock V., *A quantum Teichmüller space*, *Theor. Math. Phys.* **120** (1999), 1245–1259, math.QA/9908165.
- [6] Chekhov L., Fock V., *Quantum mapping class group, pentagon relation, and geodesics*, *Proc. Steklov Math. Inst.* **226** (1999), 149–163.
- [7] Chekhov L., Fock V., *Observables in 3d gravity and geodesic algebras*, *Czech. J. Phys.* **50** (2000) 1201–1208.
- [8] Chekhov L.O., Mazzocco M., *Isomonodromic deformations and twisted Yangians arising in Teichmüller theory*, *Advances Math.* **226**(6) (2011) 4731–4775, arXiv:0909.5350.
- [9] L. Chekhov and M. Mazzocco, *Block triangular bilinear forms and braid group action*, *Comm. Math. Phys.* **322** (2013) 49–71.
- [10] L. Chekhov and M. Mazzocco, *On a Poisson space of bilinear forms with a Poisson Lie action*, *Russ. Math. Surveys* **72**(6) (2017) 1109–1156; arXiv:1404.0988v2.
- [11] Chekhov L.O., Mazzocco M. and Rubtsov V., *Algebras of quantum monodromy data and decorated character varieties*, arXiv:1705.01447 (2017).
- [12] Chekhov, L. and Shapiro, M. *Teichmüller spaces of Riemann surfaces with orbifold points of arbitrary order and cluster variables*, *Intl. Math. Res. Notices* 2013; doi: 10.1093/imrn/rnt016. (arXiv:1111.3963, 20pp)
- [13] Coman, I., Gabella M, and Teschner J. 2015. *Line Operators in Theories of Class S, Quantized Moduli Space of Flat Connections, and Toda Field Theory*. *Journal of High Energy Physics* 2015 (10). Springer Verlag. doi:10.1007/JHEP10(2015)143. (ArXiv: 1505.05898)
- [14] Dubrovin B., *Geometry of 2D topological field theories, Integrable systems and quantum groups* (Montecatini Terme, 1993), *Lecture Notes in Math.*, **1620**, Springer, Berlin, (1996) 120–348.
- [15] Fock V.V., *Dual Teichmüller spaces* arXiv:dg-ga/9702018v3, (1997).
- [16] V. V. Fock and A. B. Goncharov, *Moduli spaces of local systems and higher Teichmüller theory*, *Publ. Math. Inst. Hautes Études Sci.* 103 (2006), 1–211, math.AG/0311149 v4.
- [17] V. V. Fock and A. B. Goncharov, *The quantum dilogarithm and representations of quantum cluster varieties*, *Inventiones Math.* **175**(2) (2008) 223–286, math.AG/0702397 v6.
- [18] V. V. Fock, and A. B. Goncharov. *Cluster ensembles, quantization and the dilogarithm II: The intertwiner*, in: *Progress in Mathematics*. Springer Basel, (2009) pp. 655–673. doi:10.1007/978-0-8176-4745-2-15
- [19] V. Fock, A. Goncharov. *Cluster X-varieties, amalgamation, and Poisson-Lie groups*. *Algebraic geometry and number theory*. (2006): 27–68.
- [20] V. V. Fock and A. A. Rosly, *Moduli space of flat connections as a Poisson manifold*, *Advances in quantum field theory and statistical mechanics: 2nd Italian-Russian collaboration* (Como, 1996), *Internat. J. Modern Phys. B* **11** (1997), no. 26–27, 3195–3206.
- [21] S. Fomin and A. Zelevinsky *Cluster algebras I: Foundations*, *J. Amer. Math. Soc.* **15** (2002), 497–529

- [22] Fomin S., Shapiro M., and Thurston D., *Cluster algebras and triangulated surfaces. Part I: Cluster complexes*, *Acta Math.* **201** (2008), no. 1, 83–146.
- [23] A. M. Gavrilik and A. U. Klimyk, *q-Deformed orthogonal and pseudo-orthogonal algebras and their representations* *Lett. Math. Phys.*, **21** (1991) 215–220.
- [24] M. Gekhtman, M. Shapiro, and A. Vainshtein, *Cluster algebra and Poisson geometry*, *Moscow Math. J.* **3**(3) (2003) 899–934.
- [25] Goldman W.M., *Invariant functions on Lie groups and Hamiltonian flows of surface group representations*, *Invent. Math.* **85** (1986) 263–302.
- [26] Henneaux M. and Teitelboim Cl., *Quantization of Gauge Systems*, Princeton University Press, 1992.
- [27] M. V. Karasev, *Analogues of objects of Lie group theory by nonlinear Poisson brackets*, *Math. USSR Izvestia* **28** (1987) 497–527.
- [28] R. M. Kashaev, *On the spectrum of Dehn twists in quantum Teichmüller theory*, in: *Physics and Combinatorics*, (Nagoya 2000). River Edge, NJ, World Sci. Publ., 2001, 63–81; math.QA/0008148.
- [29] R. M. Kaufmann and R. C. Penner, *Closed/open string diagrammatics*, *Nucl. Phys.* **B748** (2006) 335–379.
- [30] Korotkin D. and Samtleben H., *Quantization of coset space σ -models coupled to two-dimensional gravity*, *Comm. Math. Phys.* **190**(2) (1997) 411–457.
- [31] Kirill Mackenzie *General Theory of Lie Groupoids and Lie Algebroids*, *LMS Lect. Note Series* **213** (2005).
- [32] A. Molev, E. Ragoucy, P. Sorba, *Coideal subalgebras in quantum affine algebras*, *Rev. Math. Phys.*, **15** (2003) 789–822.
- [33] Nelson J.E., Regge T., *Homotopy groups and (2+1)-dimensional quantum gravity*, *Nucl. Phys. B* **328** (1989), 190–199.
- [34] Nelson J.E., Regge T., Zertuche F., *Homotopy groups and (2 + 1)-dimensional quantum de Sitter gravity*, *Nucl. Phys. B* **339** (1990), 516–532.
- [35] Postnikov A., *Total positivity, Grassmannians, and networks*, arXiv:math/0609764
- [36] Postnikov, A., Speyer, D., Williams, L., *Matching polytopes, toric geometry, and the non-negative part of the Grassmannian*, *Journal of Algebraic Combinatorics* **30** (2009), no. 2, 173–191.
- [37] A. Reyman and M. Semenov-Tian-Shansky, *Group-theoretical methods in the theory of finite-dimensional integrable systems*. Encyclopaedia of Mathematical Sciences, vol.16, Springer, Berlin, 1994 pp.116–225.
- [38] Schrader, G., Shapiro, A. *A cluster realization of $U_q(sl_n)$ from quantum character varieties*. *Invent. math.* **216**, 799–846 (2019). <https://doi.org/10.1007/s00222-019-00857-6>
- [39] G. Schrader and A. Shapiro, *Continuous tensor categories from quantum groups I: algebraic aspects*, arXiv:1708.08107.
- [40] G. Schrader and A. Shapiro, *Private communication*.
- [41] Ugaglia M., *On a Poisson structure on the space of Stokes matrices*, *Int. Math. Res. Not.* **1999** (1999), no. 9, 473–493, <http://arxiv.org/abs/math.AG/9902045> math.AG/9902045.
- [42] A. Weinstein, *Coisotropic calculus and Poisson groupoids*, *J. Math. Soc. Japan* **40**(4) (1988) 705–727.
- [43] M. Yakimov, *Symplectic leaves of complex reductive Poisson–Lie groups*, *Duke Math. J.* **112** (2002) 453–509.